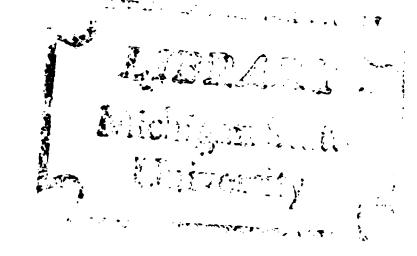
TRANSFER COEFFICIENTS AND
HETEROGENEOUS RATE CONSTANTS
FOR CJ(II) IN VARIOUS SUPPORTING
ELECTROLYTES EVALUATED BY PHASE-ANGLE
MEASUREMENTS WITH A MODIFIED
A. C. POLAROGRAPH

Thasts for the Dogree of Ph. D. MICHIGAN STATE UNIVERSITY Joseph Karl Frischmann 1966



This is to certify that the

thesis entitled

TRANSFER COEFFICIENTS AND HETEROGENEOUS RATE
CONSTANTS FOR Cd(II) IN VARIOUS SUPPORTING
ELECTROLYTES EVALUATED BY PHASE-ANGLE
MEASUREMENTS WITH A MODIFIED
A. C. POLAROGRAPH
presented by

Joseph Karl Frischmann

has been accepted towards fulfillment of the requirements for

<u>Ph.D.</u> degree in Chemistry

Major professor

Date March 7, 1966



ABSTRACT

TRANSFER COEFFICIENTS AND HETEROGENEOUS RATE CONSTANTS FOR Cd(II) IN VARIOUS SUPPORTING ELECTROLYTES EVALUATED BY PHASE-ANGLE MEASUREMENTS WITH A MODIFIED A. C. POLAROGRAPH

by Joseph Karl Frischmann

An improved a.c. polarograph was constructed. Its general features are those of an instrument constructed by Smith (37). The following modifications were introduced.

A low-gain operational amplifier was interposed between the cathode bias of the potentiostat and the tuned amplifier. This assured maintaining a virtual ground at the input of the cathode bias so that a 5mv a.c. potential could be accurately placed between the reference and at the indicating electrodes at all frequencies employed.

Electrochemical kinetic parameters are difficult to evaluate from alternating current measurements. These parameters are more simply and directly evaluated from phase-angle measurements. An improved phase-angle measuring circuit was designed and incorporated.

With a test RC series circuit constructed from components with 1% tolerance, measured phase-angles agreed with calculated values to within 1% through the frequency ranges of 30 to 250cps and 300 to 1200cps.

Transfer coefficients evaluated for the reduction of 1.0mM Cd(II) at the dropping mercury electrode at 24 \pm 1°, for the following supporting electrolytes, 0.5M Na₂SO₄, 1.0M Na₂SO₄, 0.5M H₂SO₄, 1.0M H₂SO₄, 1.0M NaClO₄, 1.0M HClO₄, 1.0M KNO₃, 1.0M HCl, 1.0M NaCl, 1.0M KCl were: 0.21, 0.20, 0.27, 0.24, 0.31, 0.26, 0.50, 0.42, 0.46, 0.44 respectively and the values for the heterogeneous rate constants, $k_h^{'}$, for the same order of the above supporting electrolytes were: 0.076, 0.063, 0.14, 0.12, 0.34, 0.25, 0.63, 0.94, 1.2, 1.2, cm/sec respectively.

Straight line $\cot \Phi - \omega^2$ plots, with intercepts $\cot \Phi = 1$, extrapolated to zero frequency, were obtained through the frequency range 30-1100cps for all supporting electrolytes containing Cd(II).

Linearity in the above plot, and agreement between experimental and calculated cot ϕ values, employing an appropriate equation derived for the electrode process

$$0 + ne \rightarrow R$$

is evidence that the electrode process is only diffusion and charge-transfer controlled.

The order of double-layer capacitance for anions of the various supporting electrolyte solutions at a d.c. potential of 0.6v vs SCE was as follows: $Cl > NO_3 > ClO_4 > SO_4$. This order parallels the order of adsorbabilities of the above anions on mercury.

The decrease in heterogeneous rate constants for the reduction of Cd(II) in the above supporting electrolytes parallels the decrease in double-layer capacitance.

TRANSFER COEFFICIENTS AND HETEROGENEOUS RATE CONSTANTS FOR Cd(II) IN VARIOUS SUPPORTING ELECTROLYTES EVALUATED BY PHASE-ANGLE MEASUREMENTS WITH A MODIFIED A. C. POLAROGRAPH

Ву

Joseph Karl Frischmann

A THESIS

Submitted to
Michigan State University
in partial fulfillment of the requirements
for the degree of

DOCTOR OF PHILOSOPHY

Department of Chemistry

(3), 1

ACKNOWLEDGMENTS

The author gratefully expresses his appreciation to Dr. Andrew Timnick for his guidance and counsel extended throughout the investigation.

Recognition is also due Dr. Richard Nicholson for his many helpful suggestions and discussions, James McLean and John Holland for their valuable technical assistance.

The author is grateful to the Socony Mobil Oil Company, the National Science Foundation, and to the Department of Chemistry for financial aid.

Special thanks go to my wife, Mary, for her encouragement and understanding throughout graduate school.

* * * * * * * * * *

VITA

Name: Joseph Karl Frischmann

Born: September 20, 1937 in Milwaukee, Wisconsin

Academic Career: Rufus King High School

Milwaukee, Wisconsin

(1951 - 1955)

Marquette University Milwaukee, Wisconsin

(1955-1961)

Michigan State University

East Lansing, Michigan

(1961-1966)

Degrees Held: B. S. Marquette University (1959)

M. S. Marquette University (1961)

TABLE OF CONTENTS

Pa	ige
INTRODUCTION	1
THEORETICAL	7
EXPERIMENTAL	20
Instrumentation	21 31 33 34 35 39 39 40 41
DISCUSSION OF RESULTS	43
Evaluation of E_1 , E_1^R , E_3 and D_0	44 46 50 54
SUGGESTED FURTHER WORK	69
SUMMARY AND CONCLUSIONS	71
IJTERATURE CITED	74

LIST OF TABLES

TABLE		Page
I.	E_{1}^{R} , i and D_{0} Values for 1.0mM Cd(II) in Various Supporting Electrolytes	45
	Variation of E_1^R with Concentration and Type of Electrolyte in Isolation Compartment. Sample Solution is 1.0mM Cd(II) in 1M HClO $_4$.	47
III.	Variation of C _{d.1} . and Phase-Angle Correction with Changing E _{d.C} . for 1.0mM Cd(II) in 1M Na ₂ SO ₄ at 822cps	51
IV.	Values of the Transfer Coefficient, α , Obtained from Slope Measurements for 1.0mM Cd(II) in Various Supporting Electrolytes	52
V.	Values of the Transfer Coefficient, α , for 1.0mM Cd(II) in Various Supporting Electrolytes	53
VI.	Values for the Heterogeneous Rate Constant, k_h , for 1.0mM Cd(II) in Various Supporting Electrolytes. Values for Cd.1. and Rt, for Electrode Used are Included	56
VII.	Effect of Cd(II) Concentration on the Heterogeneous Rate Constant, $k_h^{'}$	57
VIII.	Tabulation of Heterogeneous Rate Constants and Transfer Coefficient. Values Determined by Various Investigators	64



LIST OF FIGURES

FIGUR	E	Page
1.	Variation of cot ϕ with changing d.c. potential for 1) preceding, 2) no, 3) following first order chemical reaction	17
2.	Essential components for an a.cd.c. polarograph	24
3.	Schematic of the \pm d.c. potential source	25
4.	Schematic of the a.c. potential source	26
5.	A.c. signal measuring component	28
6.	Schematic for full-wave rectifier	29
7.	Schematic of circuit for detecting phase dif- ference between polarographic and reference signal	30
8.	Schematic of potentiostat switched to the calibrating mode	32
9.	Electrolysis cell	36
10.	Auxiliary and reference electrode	37
11.	Typical a.c. polarogram for 1.0mM Cd(II) in 1M Na ₂ SO ₄ at 33.8cps	48
12.	Typical a.c. polarogram for 1.0mM Cd(II) in 1M Na ₂ SO ₄ at 822cps	49
13.	Variation of cot $^{\varphi}$ with changing a.c. frequency for 1mM Cd(II) in various supporting electrolytes	55
14.	Variation of cot $^{\circ}$ with changing Ed.c. at 34.8 cps for 1mM Cd(II) in 0.5M Na ₂ SO ₄	59
15.	Variation of cot ϕ with changing Ed.c. at 825 cps for 1.0mM Cd(II) in 0.5M Na ₂ SO ₄	60

LIST OF FIGURES - Continued

FIGURE	Ξ	Page
16.	Variation of cot ϕ with changing Ed.c. at 34.4cps for 1.0mM Cd(II) in 0.5M H ₂ SO ₄	61
17.	Variation of cot $^{\varphi}$ with changing E _{d.C.} at 828 cps for 1mM Cd(II) in 0.5M H ₂ SO ₄	62
18.	Variation of double-layer capacitance with changing applied d.c. potential for various supporting electrolytes	65
19.	Variation of double-layer capacitance with changing applied d.c. potential for various supporting electrolytes	66

INTRODUCTION

For a long time after the discovery of electrochemical phenomena, investigators were concerned with gross effects such as the relationship between the quantity of electricity consumed and the amount of electrochemical reaction which occurred at electrodes, or the relationship between the potential of electrodes and the concentration and nature of species influencing the potential, or the relationship between the number and species of ions in solution and amount of current conducted by the solutions. Later efforts were directed to the examination of many aspects of these phenomena and were put on sound theoretical basis through classical thermodynamics. Even though good agreement between the magnitude of some electrical quantity and the kinds and number of species was obtained when expected and measured quantities were compared, still no exact explanations of processes at electrodes were revealed through the above efforts.

During the 1920's, the attention of some electrochemists was directed to behavior of microelectrodes resulting in the development of polarography by Heyrovsky in 1924. Now the electrochemists began to consider the individual contributions of electron transfer, mass transfer to the electrode, and removal of reaction product to the total electrode process. Up to the early 1950's, d.c. polarography was exploited for analytical applications, for determining whether an electrode process was reversible, for the evaluation of

the number of electrons involved in a reduction or oxidation step, for the determination of whether or not stepwise reduction occurred for complexation studies, or for the
evaluation of diffusion coefficients.

Since many electrode processes were irreversible, causes for irreversibility had to be identified and attention was now drawn to kinetic effects. Pioneers in this field among others were Eyring and Koutecky.

In the application of the absolute rate theory to electrode processes, Eyring (21) developed the general current-potential relationship for the reaction

$$O + ne \longrightarrow R$$
.

The equation is

$$i(t) = n FAk_{h}' \{C_{O} \exp \left(-\frac{nF}{RT} \alpha(E(t)-E^{O})\right) - C_{R} \exp \left(\frac{(1-\alpha)nF}{RT} (E(t)-E^{O})\right)$$

in which i(t) is the current flowing at time t, at an applied potential E(t), E^{O} is the standard electrode potential, C_{O} and C_{R} are the surface concentrations of oxidized and reduced species, n, F, R, T, have their usual significance and α , the transfer coefficient, and k_{h} , the heterogeneous rate constant, are the kinetic parameters.

The heterogeneous rate constant, $k_{\rm h}^{'}$ in cm/sec, is the rate constant for charge-transfer at the standard electrode

potential. The following is a simple explanation of the significance of α as well as its indirect definition.

For an electrochemical reaction to occur in a potential field an energy barrier must be overcome. This existing potential will favor the reaction in one direction and hinder the reaction in the opposite direction. If the potential that favors the forward reaction is αE , then $(1-\alpha)E$ is the potential that favors the back reaction, so α simply is the fraction of the existing potential which drives the reaction in one direction.

Koutecky (26) derived equations for irreversible processes which indicated that α and $k_h^{'}$ could be evaluated by d.c. polarography but applications were limited. To extend the evaluation to faster electron transfer reactions, newer electrochemical methods such as cyclic voltammetry, galvanostatic, potentiostatic, faradaic rectification, faradaic impedance, and various forms of a.c. polarography were developed.

A. c. polarography was first used in 1938 by Müller and co-workers (31) to evaluate d.c. half-wave potentials by noting the d.c. potential at which the alternating current had minimum distortion.

The first correct interpretation of the electrode process in the presence of an applied a.c. potential was reported in 1941 by Grahame (22). He concluded that the large apparent change in double-layer capacity in the

potential range between the start of the reduction of Cd(II) and up to the limiting current, was due to the electro-reduction of Cd(II) and re-dissolution of Cd in phase with the applied a.c. potential.

The earliest equations reported for the evaluation of rate constants from faradaic impedance measurements were derived independently in 1947 by Randles (34) and Ershler (19).

A more complete discussion of the developments in a.c. polarography up to 1962 is recorded in a monograph by Breyer and Bauer (8).

Until very recently, all the equations for the a.c. methods were derived for diffusion to a plane electrode. Delmastro and Smith (17, 18), have shown that all the a.c. wave equations previously derived do not adequately describe the relationship between current and kinetic parameters for electrode processes occurring at a spherical electrode. The equations for diffusion to a plane and spherical electrode are given in detail in the theoretical section.

From the theoretical expressions it becomes apparent that α and $k_h^{'}$ can be evaluated by a.c. polarography from alternating current measurements. Such currents can be measured accurately but the final evaluation of the parameters is difficult. The parameters can be more directly evaluated by measuring the phase-angle between the faradaic alternating current and the applied a.c. potential.

Experimental instruments with which exactly known, steady small amplitude a.c. potentials could be impressed between the electrodes and with which phase-angles could be accurately measured, did not exist when this study was undertaken. Furthermore, there were wide discrepancies in values of α and $k_h^{'}$ for Cd(II) reduction determined by various methods and for various supporting electrolytes or in values determined by different investigators employing similar methods (see Table VIII).

This study was undertaken to construct an instrument with which a 5 mv a.c. potential could be impressed accurately between the electrodes and with which the phase angles could be precisely measured. The capabilities of the instrument were to be tested with the evaluation of α and k_h^i for Cd(II) in various supporting electrolytes and to establish whether or not the double-layer capacitance affected directly the charge-transfer process.

THEORETICAL

Alternating current polarography is a technique in which the d.c. and a.c. potentials applied to the polarographic cell are controlled and the resulting alternating current is measured as function of the d.c. potential with the amplitude of the alternating potential held constant. With this technique only reversible and quasi-reversible electrode processes for the reaction

$$O + ne \rightarrow R$$

can be examined since irreversible processes yield no a.c. waves.

Before proceeding with the discussion of the theoretical section which will require the statement of numerous equations, the definitions of symbolism employed are tabulated below for ready reference.

A = electrode area

 α, β = mass transfer coefficients, β = (1 - α)

Cf = faradaic capacitance

 C_{i}^{*} = initial concentration of species i

 D_i = diffusion coefficient of species i

 $E_{d.C.}$ = applied d.c. potential

E^O = standard redox potential

 $E_{\frac{1}{2}}^{R}$ = reversible half-wave potential

E(t) = instantaneous value of potential

 ΔE = amplitude of the applied a.c. potential

F = Faraday's constant

erfc = error function complement

 f_i = activity coefficient of species

 ΔI = amplitude of measured first harmonic alternating current

id.c. = d.c. faradaic current component

K = equilibrium constant

 k_1, k_2 = first order chemical reaction rate constants

 k_{h} = heterogeneous rate constant for charge-transfer at E^{O}

n = number of electrons transferred

R = gas constant

Re = resistance of indicating electrode

 R_f = faradaic resistance

 r_0 = spherical electrode radius

 R_{S} = solution resistance

 R_{+} = total series resistance

T = absolute temperature

t = time

 ω = angular frequency

x = distance from the electrode surface

 $Z_f = faradaic impedance$

An ideal reversible process is one in which the chargetransfer rate is so rapid that the current is purely diffusion controlled. The expressions for the faradaic alternating current and the faradaic impedance associated with diffusion only have been derived by Breyer and Hacobian (11), Delahay and Adams (16), Matsuda (29), Tachi and Senda (40) for diffusion to a plane electrode. The expression for faradaic alternating current when $\Delta E \leq 8 \text{mv}$, and whether or not the reduced form is soluble in the electrode, is

$$I(\omega t) = \frac{n^2 F^2 A Co^* (\omega D_0)^{\frac{1}{2}} \Delta E}{4RT \cosh^2 (\frac{1}{2})} \sin (\omega t + \frac{\pi}{4})$$
 (1)

$$I(\omega t) = I_{rev.} \sin (\omega t + \frac{\pi}{4})$$
 (2)

in which

$$j = \frac{nF}{RT} \left(E_{d,C} - E_{\frac{1}{2}}^{R} \right)$$
 (3)

for an applied potential

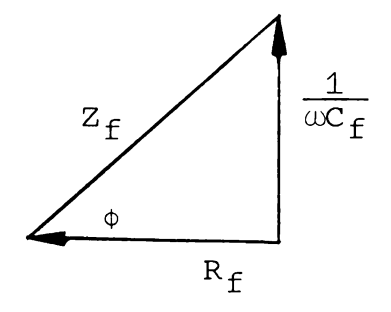
$$E(t) = E_{d,C} - \Delta E \sin(\omega t)$$
 (4)

For the faradaic impedance, the expression is

$$Z_{f} = \frac{4RT \cosh^{2}(j/2)}{n^{2}F^{2}AC_{0}^{*}(\omega D_{0})^{\frac{1}{2}}}$$

$$(5)$$

The faradaic impedance can be considered equivalent to a series RC circuit. The phase relationship for a series network is as follows



 R_{f} and C_{f} are the resistive and capacitative components of the faradaic impedance and from the above diagram, it is obvious that

$$Cot \Phi = R_f \omega C_f$$
 (6)

and

$$(R_f)^2 + (\frac{1}{\omega C_f})^2 = (Z_f)^2$$
 (7)

For an ideal reversible process the alternating current leads the applied alternating potential by 45° (cot φ = 1), then

$$R_{f} = \frac{1}{\omega C_{f}} = \frac{4RT \cosh^{2} (j/2)}{n^{2}F^{2}AC_{0}*(2\omega D_{0})^{\frac{1}{2}}}$$
(8)

In a recent study by Delmastro and Smith (18), for the influence of spherical diffusion on the alternating current polarographic wave, the following more rigorous expression for $I(\omega t)$ was developed for the reduced form being soluble in the electrode:

$$I(\omega t) = I_{rev} \cdot \left[1 + \frac{D_0^{\frac{1}{2}} + D_R^{\frac{1}{2}}}{e^j D_0^{\frac{1}{2}} - D_R^{\frac{1}{2}}} \left[1 - \exp(b^2 t) \operatorname{erfc}(bt^{\frac{1}{2}}) \right] \right]$$

$$\sin (\omega t + \frac{\pi}{4}) \quad (9)$$

or simply

$$I(\omega t) = I_{rev.} H_{s} \sin \left(\omega t + \frac{\pi}{4}\right)$$
 (9a)

and

$$b = \frac{e^{j} D_{0}^{\frac{1}{2}} - D_{R}^{\frac{1}{2}}}{r_{0} (1 + e^{j})}$$
 (10)

Equation (9) differs from equation (1) by the quantities enclosed in the large brackets and these quantities constitute a correction term, (H_S) , to account for the difference between diffusion to a spherical electrode and a plane electrode.

A quasi-reversible electrode process is one in which the current is diffusion and charge-transfer controlled. The equations which follow were derived with the assumption that the d.c. process was reversible.

Matsuda (30) has derived rigorous equations for the quasi-reversible system. Smith (39) slightly modified Matsuda's equations for the controlled a.c. potential technique.

Smith's expression for the faradaic alternating current for a plane electrode is

$$I(\omega t) = I_{rev}.F(t) \left[\frac{2}{1 + (1 + \frac{(2\omega)^{\frac{1}{2}}}{\lambda})^2} \right]^{\frac{1}{2}} \sin(\omega t + \phi)$$

$$(11)$$

for which I_{rev} is defined by equations (1) and (2), and

$$F(t) = 1 + \left[\frac{(\alpha e^{-j} - \beta) D^{\frac{1}{2}} Q_0(t)}{k_h} \right]$$
 (12)

$$\lambda = \frac{k_h f}{D^2} \left[e^{-\alpha j} + e^{\beta j} \right]$$
 (13)

$$\Phi = \cot^{-1}\left(1 + \frac{(2\omega)^{\frac{1}{2}}}{\lambda}\right) \tag{14}$$

$$Q_{0}(t) = \frac{i_{d.c.}(t)}{nFA C_{0}* D_{0}^{2}}$$
 (15)

$$f = f_0^{\beta} f_R^{\alpha}$$
 (16)

$$D = D_0^{\beta} D_R^{\alpha} \tag{17}$$

Delmastro and Smith (18) also considered spherical diffusion for the quasi-reversible case and arrived at an expression which has the same form as equation (11) and equations (13)-(17) pertain. In the new expression F(t) is identical with the spherical correction term, $H_{\rm S}$, defined in equations (9) and (9a).

Evaluation of the heterogeneous rate constant, k_h , and mass transfer coefficients, (α , β), by either equation (10) or Delmastro and Smith's (18) modified equation from an a.c. polarogram would be extremely cumbersome. However, the mere knowledge of Φ , the phase-angle, regardless of whether diffusion is to a plane or spherical electrode, allows one to readily determine the desired parameters as will be shown from the following considerations.

By algebraic manipulation of equations (13), (3) and (14), one obtains

cot
$$\phi = 1 + \frac{(2 \omega D)^{\frac{1}{2}}}{k_h f(e^{-\alpha j} + e^{\beta j})}$$
 (18)

Equation (18) predicts that a plot of cot ϕ versus $\omega^{\frac{1}{2}}$ at a fixed d.c. potential should yield a straight line with an intercept at cot ϕ = 1 and a

slope =
$$\frac{(2 \text{ D})^{\frac{1}{2}}}{k_{h}^{'} (e^{-\alpha j} + e^{\beta j})}$$
 (19)

where

$$k_h = k_h f . (20)$$

The apparent heterogeneous rate constant, k_h , uncorrected for activity coefficients is the term calculated in this work.

For the special case where j=0, that is, the applied d.c. potential is equal to the reversible half-wave potential, one can calculate from the slope and D, defined in equation (17), a value of k_h^{\dagger} by the following simple expression

$$k_{h} = \frac{(D)^{\frac{1}{2}}}{\text{slope } (2)^{\frac{1}{2}}}$$
 (21)

There are two methods for obtaining the mass transfer coefficients. In the first method, as equation (18) predicts, cot ϕ will exhibit a maximum when the term $(e^{-\alpha j} + e^{\beta j})$ is at a minimum. This will occur at

$$E_{d.c.} = E_{\frac{1}{\beta}}^{R} + \frac{RT}{nF} \ln \frac{\alpha}{\beta}$$
 (22)

The second method consists of determining the slopes resulting from the plot of cot Φ versus $\omega^{\frac{1}{2}}$ at two different d.c. potentials. The value of α can be determined by

$$\alpha = \frac{1}{2} - \frac{2.303}{2(j_2 - j_1)} \log \frac{\text{slope}_1}{\text{slope}_2}$$
 (23)

One can obtain the reversible faradaic alternating current equation (1) from equation (11) by letting \mathbf{k}_h approach ∞ .

The quantities in the latter equation defined by equations (12), (13), (14) will then go to 1, ∞ , and $\frac{\pi}{4}$ respectively. A form of equation (11) for spherical diffusion reduces to equation (9) when k_h approaches ∞ .

Smith (37) has also derived equations for frequency and potential effects on phase-angles for systems with preceding or following first order chemical reactions accompanying the charge-transfer.

For the system with a preceding chemical reaction,

$$Y \stackrel{k_1}{\rightleftharpoons} 0 + ne \stackrel{\longrightarrow}{\rightleftharpoons} R$$

the cot Φ was shown to be

$$\cot \Phi = \frac{\left(\frac{2\omega}{\lambda}\right)^{\frac{1}{2}} + \frac{1}{1+e^{j}} \left\{ \frac{1}{1+K} \left[\frac{(1+g^{2})^{\frac{1}{2}} + g}{1+g^{2}} \right]^{\frac{1}{2}} + \frac{K}{1+K} + e^{j} \right\}}{\frac{1}{1+e^{j}} \left\{ \frac{1}{1+K} \left[\frac{(1+g^{2})^{\frac{1}{2}} - g}{1+g^{2}} \right]^{\frac{1}{2}} + \frac{K}{1+K} + e^{j} \right\}}$$
(24)

where

$$K = \frac{k_1}{k_2} \tag{25}$$

$$g = \frac{k_1 + k_2}{\omega} \tag{26}$$

It can be seen that either large K value or high frequency potential will reduce equation (24) to

$$\lim_{K \to \infty} \cot \Phi = \lim_{\phi \to \phi} \cot \Phi = 1 + \frac{(2\omega)^{\frac{1}{2}}}{\lambda}$$
(27)

and at low frequencies, equation (24) reduces to the following:

$$\lim_{g \to \infty} \cot \Phi = 1 + \frac{(2\omega)^{\frac{1}{2}}}{\lambda} \left(\frac{1 + e^{j}}{1 + K} + e^{j} \right)$$

$$\omega \neq 0$$
(28)

By performing an experiment at high frequencies, λ can be evaluated (equation (27)). Once λ is known, a low

frequency experiment performed under conditions so that j = 0, K may be evaluated.

For the system with a following chemical reaction

$$0 + ne \longrightarrow R \xrightarrow{k_2} Y$$

the cot ϕ was derived to be

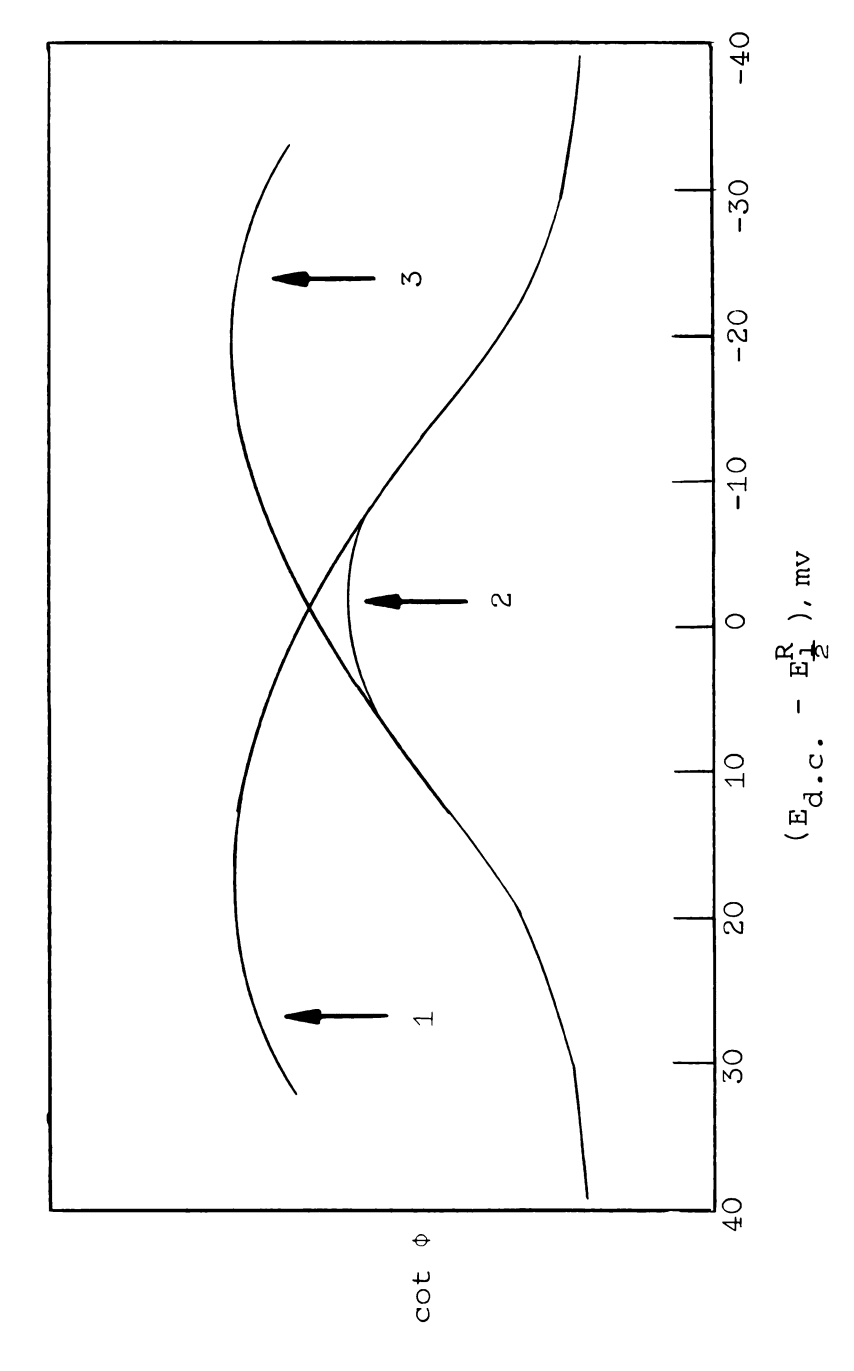
$$\cot \phi = \frac{\frac{(2\omega)^{\frac{1}{2}}}{\lambda} + \frac{1}{(1+e^{j})} \left\{ \frac{e^{j}}{1+K} \left[\frac{(1+q^{2})^{\frac{1}{2}}+q}{1+q^{2}} \right]^{\frac{1}{2}} + \frac{Ke^{j}}{1+K} + 1 \right\}}{\frac{1}{1+e^{j}} \left\{ \frac{e^{j}}{1+K} \left[\frac{(1+q^{2})^{\frac{1}{2}}-q}{1+q^{2}} \right]^{\frac{1}{2}} + \frac{Ke^{j}}{1+K} + 1 \right\}}$$
(29)

where K and g are defined by equations (25) and (26) respectively. When the limits $K \to \infty$, $g \to 0$ are imposed equation (29) reduces to equation (27) and when $g \to \infty$, $\omega \neq 0$,

lim cot
$$\phi = 1 + \frac{(2\omega)^{\frac{1}{2}}}{\lambda} \left(\frac{1 + e^{j}}{\frac{Ke^{j}}{1 + K}} \right)$$
 (30)

As for the previous system, K can be evaluated by high and low frequency experiments.

Equations(24) and (29) do not predict a linear relationship between cot ϕ and $\omega^{\frac{1}{2}}$ and non-linearity in a cot ϕ - $\omega^{\frac{1}{2}}$ plot indicates that processes in addition to diffusion and charge-transfer are occurring. Since both systems yield similar non-linear plots, it is not possible to distinguish between the systems on this basis. The two systems can be distinguished by the different variation in cot ϕ with d.c. potential when a constant, low-frequency potential is applied. This difference is illustrated by Figure 1.

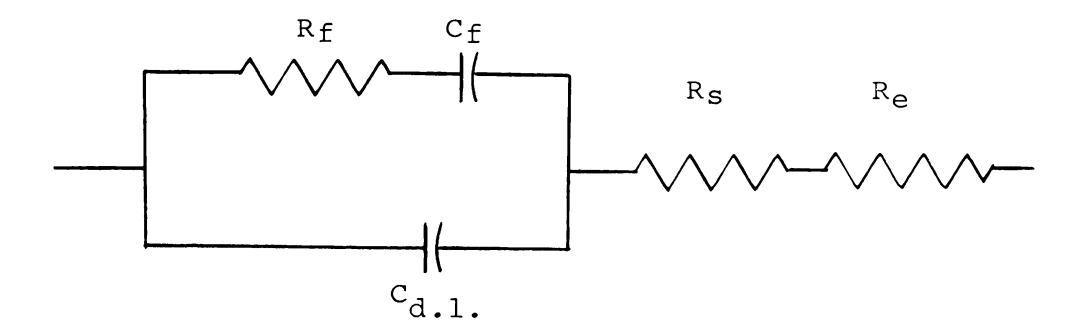


Variation of cot Φ with changing d.c. potential for 1) preceding, 2) no, 3) following first order chemical reaction; $\alpha=0.5,\ k_h,\ finite,\ K=1.$ Figure 1.

The assumptions which were made for the derivations of equations pertaining to the faradaic current and phase-angle dependence are:

- (1) Fick's law (13) can be applied to each species.
- (2) The absolute rate equation (21) can be applied to the electrode reaction kinetics.
- (3) Charge-transfer involves one rate-determining step.
- (4) Diffusion and chemical reaction are the sole means of mass transfer.
- (5) Adsorption effects are negligible.

The above equations are also derived solely for the faradaic current, that is, the current arising from the electrochemical reaction. However, the current from the polarographic cell consists of the faradaic current and double-layer capacitative currents. The polarographic current must pass through resistance offered by the solution and the indicating electrode.



The above is an equivalent circuit for the polarographic cell. R_{f} and C_{f} are the faradaic impedances, $C_{\mathrm{d.l.}}$ is the

capacity of the double-layer, $R_{\rm S}$ is the resistance of solution, and $R_{\rm e}$ is the resistance of the indicating electrode.

To evaluate kinetic parameters for the electrode processes the faradaic phase-angle must be known. Any measured phase-angle must be corrected for the effects of double-layer capacitance and total series resistance. Bauer and Elving (2) derived the following relationship to calculate the phase-angle of the faradaic current:

$$\cot \Phi = \frac{\frac{\Delta I}{\Delta E} (\cos \Phi' - \frac{\Delta I}{\Delta E} R_{t})}{\frac{\Delta I}{\Delta E} \sin \Phi' - \omega C_{d.1.} (1 + (\frac{\Delta IR_{t}}{\Delta E})^{2} - \frac{2\Delta IR_{t}}{\Delta E} \cos \Phi')}$$
(31)

where

- ΔI is the amplitude of the alternating current measured.
- ΔE $\,$ is the amplitude of the alternating potential applied.
- $\boldsymbol{\varphi}^{\boldsymbol{\prime}}$ is the phase-angle measured between the alternating current measured and the alternating potential applied.
- ω is the angular frequency.

C_{d.l.} is the capacity of the double-layer.

 $R_t = R_s + R_e$ (total series resistance).

EXPERIMENTAL

Instrumentation

The instruments employed in this investigation are as follows:

A Sargent S-30260 potentiometer was used to measure all d.c. potentials applied to the cell.

A Tektronix Model 502 oscilloscope was employed to measure the amplitude of the a.c. potential applied to the cell and to monitor the tuning of the frequency sensitive amplifier.

The Sargent Model M.R. and S.R. one second full scale deflection recorders were employed to measure the maximum d.c. currents, rectified a.c. currents, and signal proportional to the phase-angle.

A Hewlett-Packard Model 202A signal generator provided all a.c. potentials.

A Hewlett-Packard Electronic Counter Model 521A was employed to calibrate the frequency of the Hewlett-Packard signal generator.

A Philbrick Model R-300 power-supply provided up to 300ma of \pm 300 v.d.c.

A Chicago-Stancor transformer was used as a 20 ampere, 6.3v filament supply.

The A. C. Polarograph

Previous to 1963, a.c. polarographs were constructed using conventional circuitry but during that year there was

considerable activity in exploiting operational amplifiers as elements in electrochemical instrumentation (33). With experience gained at the Oak Ridge National Laboratory (20) during the summer of 1963, the construction of the instrument used in this study was undertaken.

The potentiostat of the instrument was essentially that designed by Kelley, Jones, Fisher (25). It employed a Deford follower (12) which places a high impedance path at the reference electrode so that current flows between the indicating electrode and auxiliary electrode instead of between the indicating electrode and the reference electrode. This type of potentiostat was similar to one constructed by Smith (37), but instead of proceeding on to the tuned amplifier as Smith had done, another low-gain operational amplifier was interposed between the cathode bias (amplifier C, Figure 2) and the tuned amplifier (amplifier F, Figure 5).

Since Smith's (37) phase-angle detecting circuit had high and low level current limitation, this part of the instrument was modified by eliminating the diodes, which broke down at high currents, from the feedback loop. The operational amplifier, now at open loop performed simply as a voltage detector which responded to input signals from 50mv to 100v. Thus the high level current limitation of Smith circuit was overcome without sacrifice of low current sensitivity. Details of the modified phase-angle detector will be discussed subsequently in more detail.

Conventional circuitry for full-wave rectification and signal recording was employed. Pertinent details of the components comprising the instrument will now be discussed.

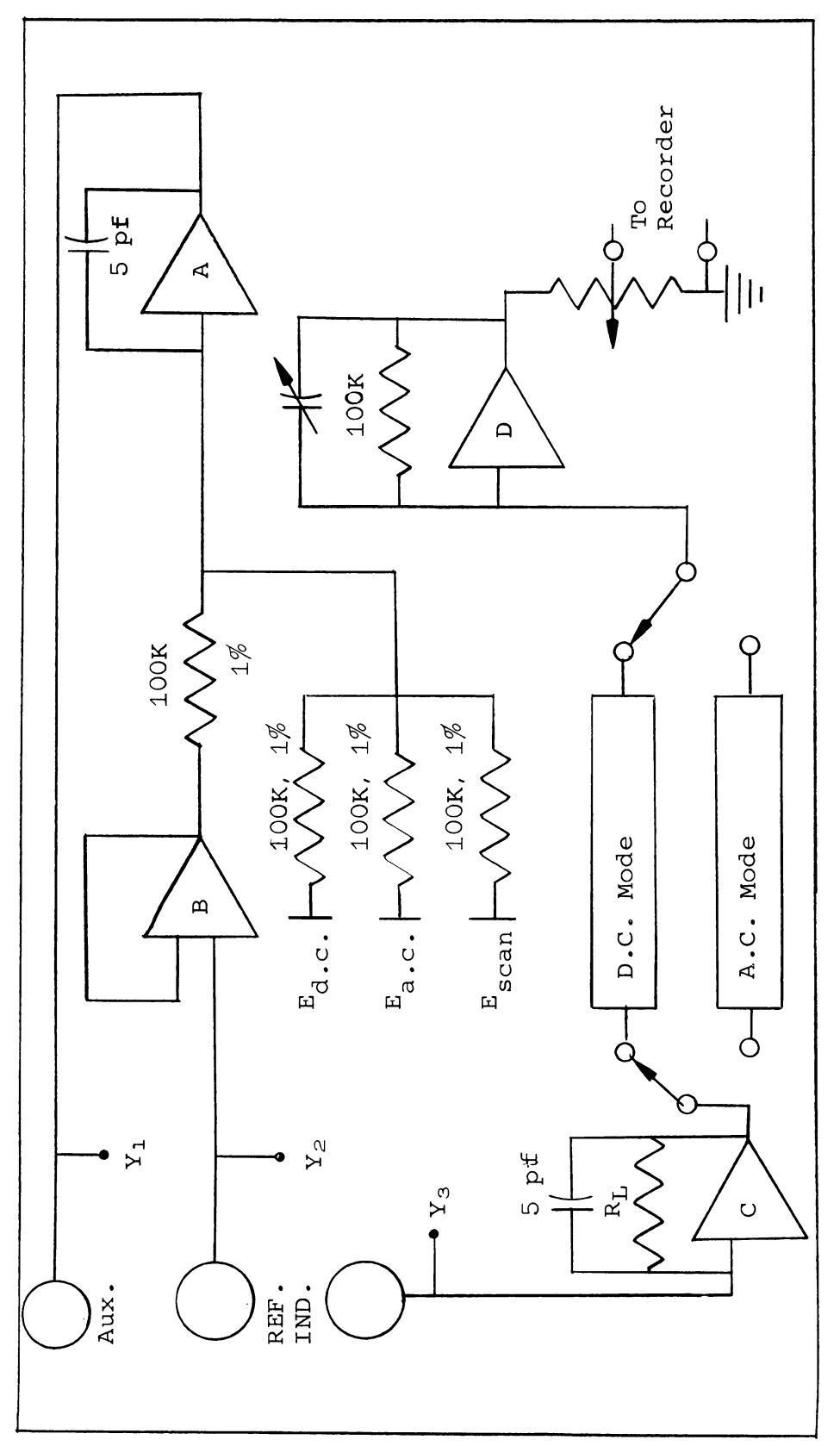
Figure 2 shows a block diagram of the instrument. The potentiostat consists of operational amplifiers A, B, and C. A.c. mode and d.c. mode are the units utilized for measuring a.c. or d.c. signals. Amplifier D attenuates the signal for recording.

The constructional details for the stable d.c. potential source to supply the $E_{\rm d.c.}$ are shown in Figure 3. From 0 to \pm 3 volts could be obtained from this source with the aid of the 1K Helipot. The long term instability of the supply was at most 0.1mv.

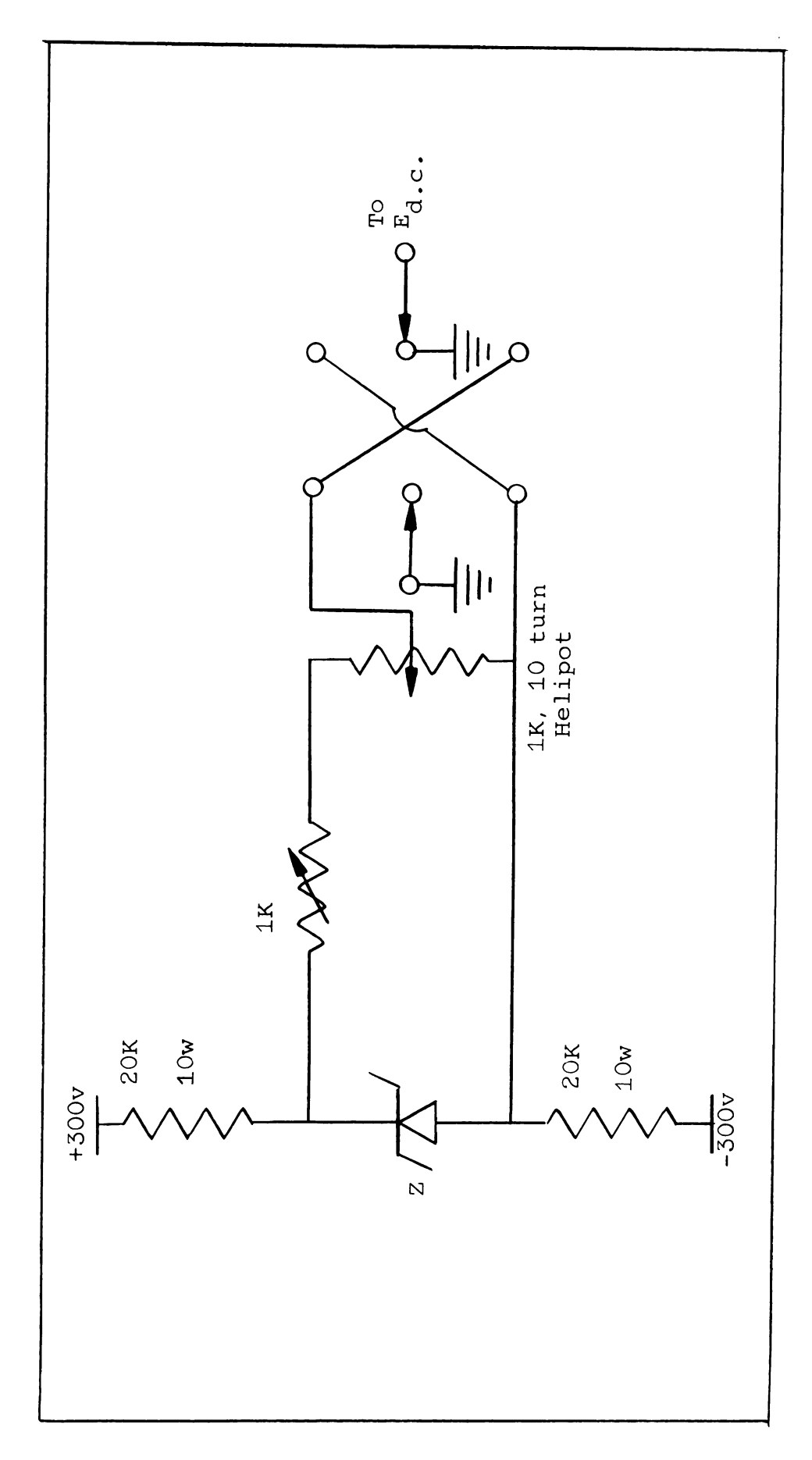
The constructional details for the $E_{\rm a.c.}$ supply are shown in Figure 4. A 1000 fold or 100 fold attenuation of the 5 volt signal from the signal generator produces 5 or 50mv across the 10 turn Helipot from which ranges of 0 to 5.00 \pm 0.05mv or 0 to 50.0 \pm 0.5mv were available. The frequency of the signal generator was calibrated and typically corresponded to within 0.6% of the dial reading in the frequency range of 30 to 1200cps.

A d.c. scanning unit, $E_{\text{d.c.}}$ scan, not used in this investigation, was also incorporated in the instrument.

To record an a.c. polarogram, a 5mv a.c. potential together with the desired d.c. potential were applied at $E_{\rm a.c.}$ and $E_{\rm d.c.}$. The output of amplifier C, related to



configuration; Aux., Ref., Ind., Auxiliary, reference and indicator electrodes Essential components for an a.c.-d.c. polarograph. Amplifiers A, C, D are Philbrick WSA-.3'S; Amplifiers B - Philbrick K2X-A, K2-P in Deford follower Y_1 , Y_2 , Y_3 see Figure 7. respectively. 2 Figure



Schematic of the \pm d.c. potential source. Z : T.I. 652CO Zener diode, 5.5v nominal. Figure 3.

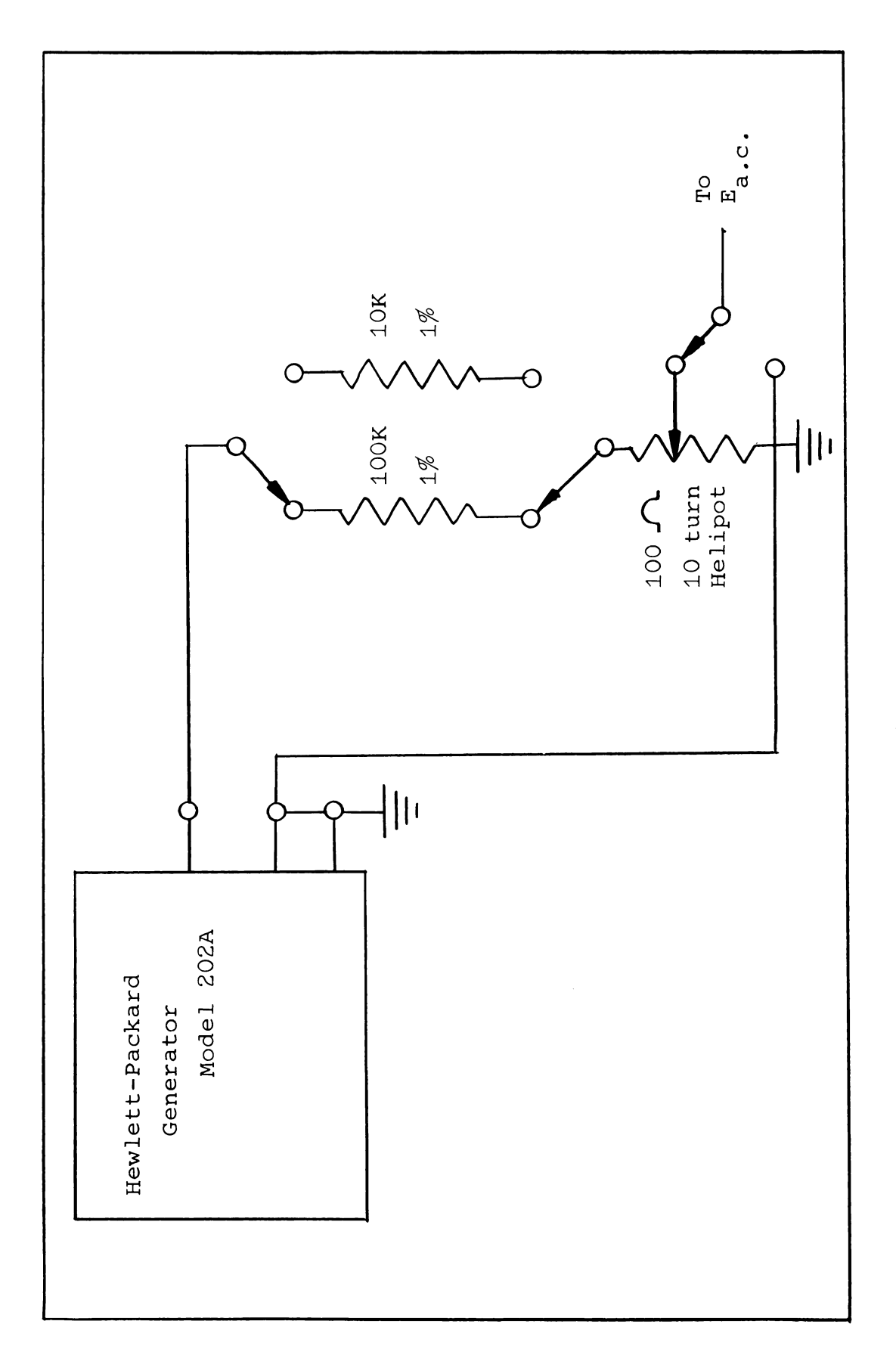


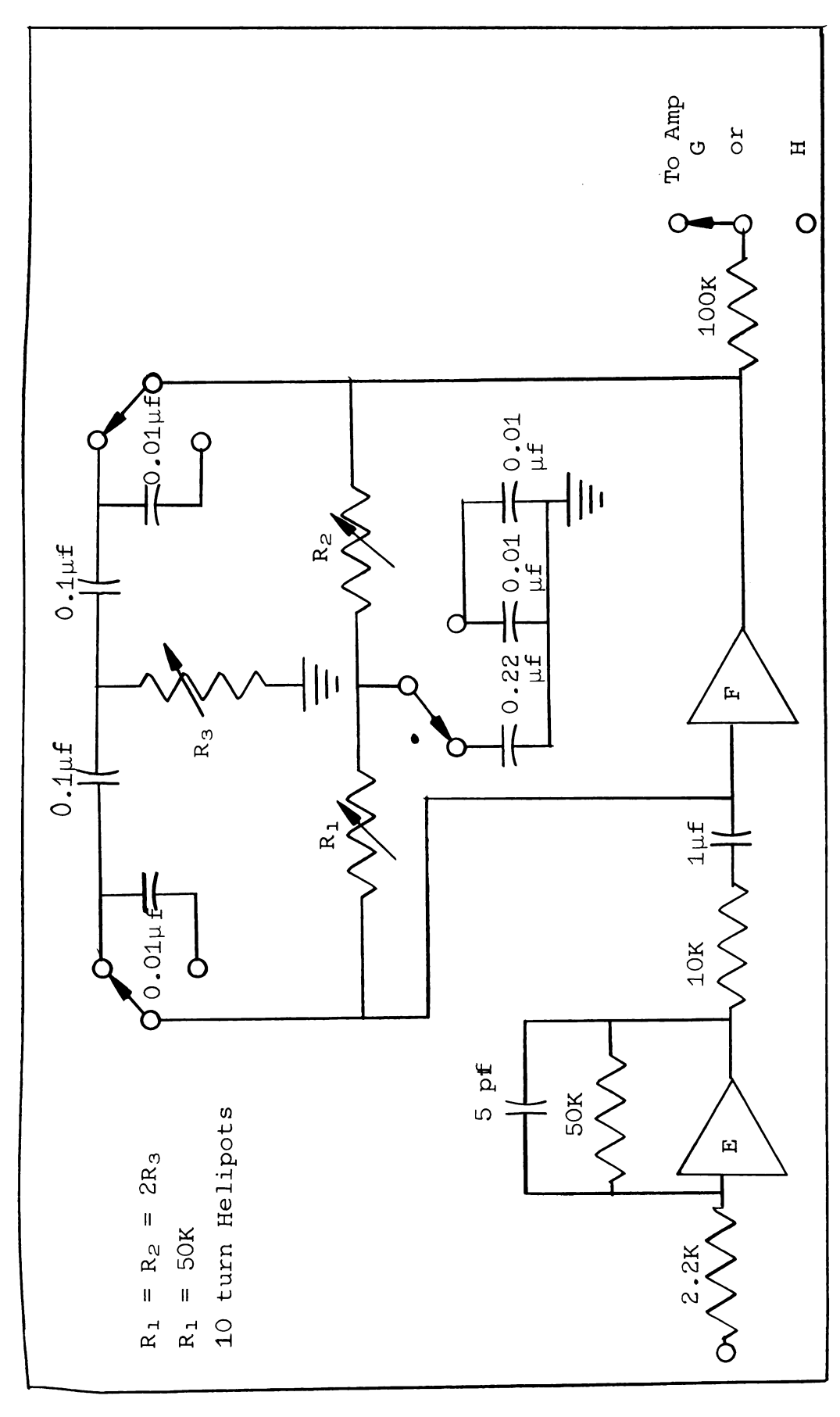
Figure 4. Schematic of the a.c. potential source.

current passing through the polarographic cell, is amplified by amplifier E (Figure 5). The use of amplifier E makes possible the gain adjustment of amplifier C so that C can maintain its input at a virtual ground at all frequencies employed. If a resistance of 5K or greater were put in the feedback loop (R_L) of amplifier C, a small a.c. potential of the frequency (> 500cps) introduced would appear at the input. This resulted in current measurement errors of about 10% and phase-angle errors of about 5° at 1000 cps. When R_L was lowered to 470 ohms, this problem was eliminated in the frequency range of 30 to 1200 cps.

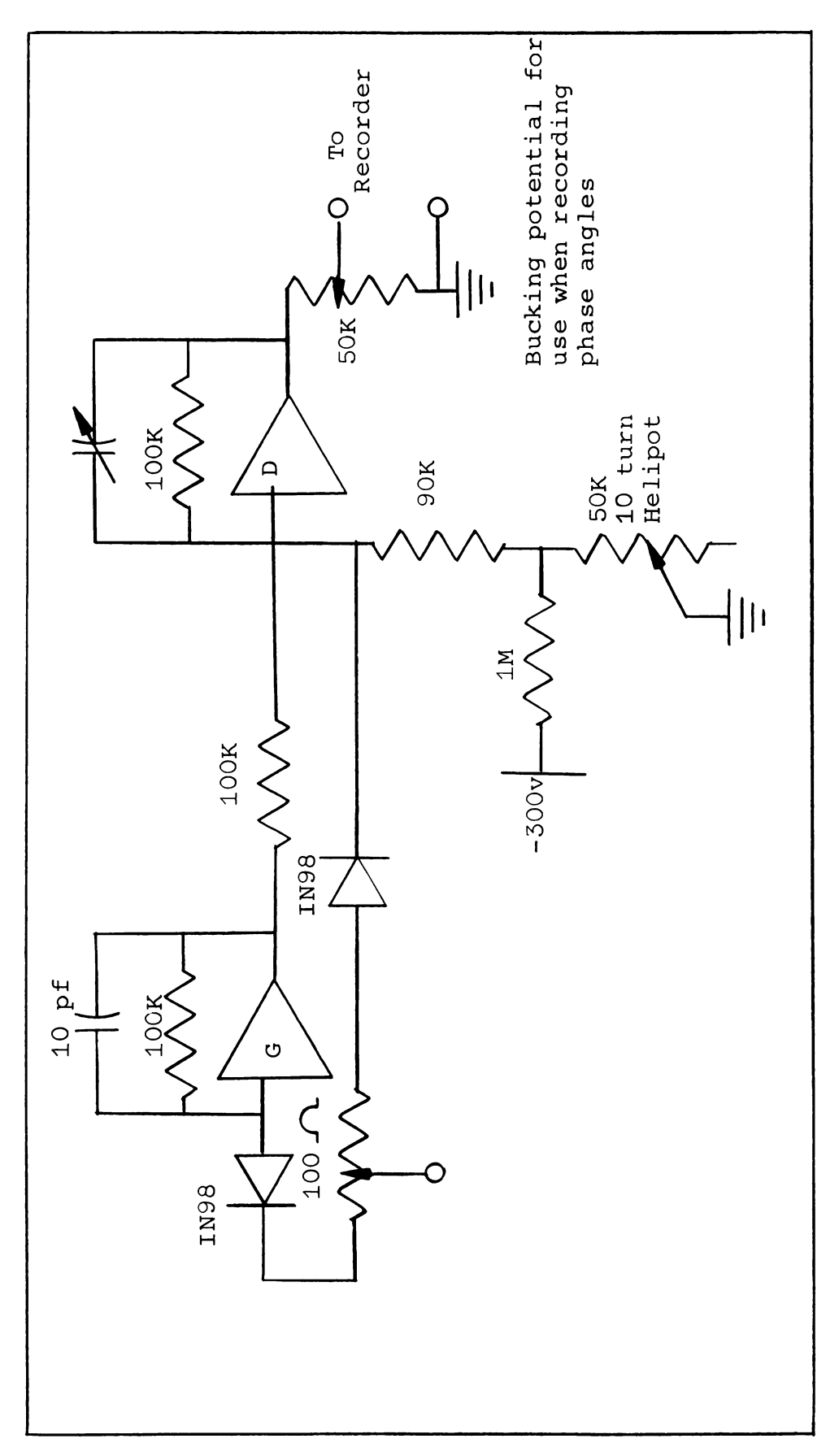
To obtain fundamental-harmonic a.c. polarograms which are undistorted by effects of extraneous a.c. signals (60cps noise or higher harmonic faradaic components) and to make phase-angle measurements, a highly frequency-selective amplifier (Figure 5, amplifier F) was introduced as an integral part of this instrument. The amplifier has two frequency ranges which enable it to amplify selectively any frequency in the range of 30 to 250cps or 300 to 2500cps.

The signal from amplifier F is rectified by the circuit shown in Figure 6 and recorded.

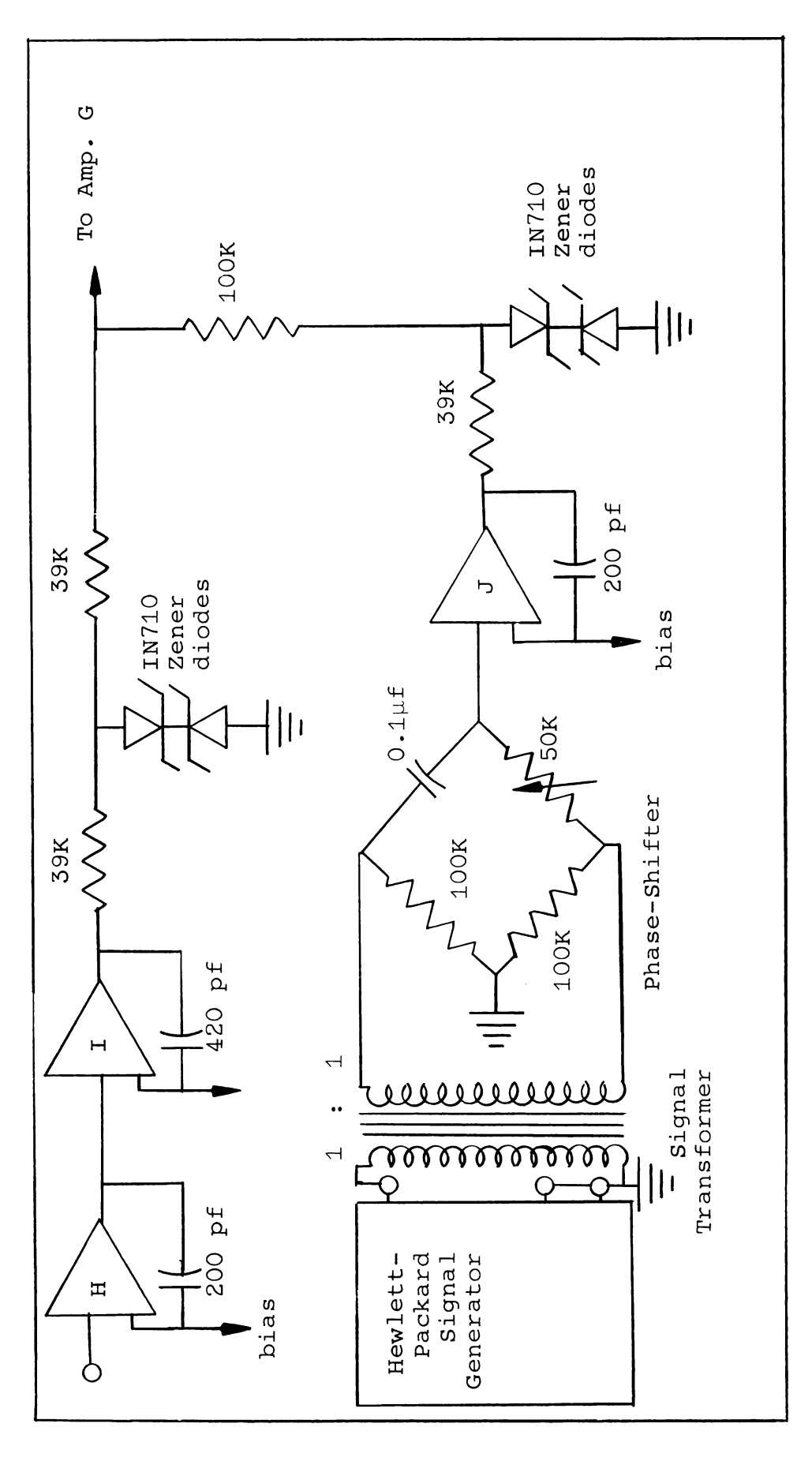
In Figure 7 amplifiers H, I, and J are high gain limiting voltage detectors which give square wave outputs of the same frequency and phase as their a.c. input signals. The amplitude of these square waves after clipping with back-to-back Zener diodes, is independent of the amplitude of the original a.c. signal.



E and F are Philbrick SK-2V and WSA-3 amplifiers respectively; G for current measurement; H for phase-angle measurement. A.c. signal measuring component. 5 Figure



a Philbrick K2X-A amplifier. ı. ტ Schematic for full-wave rectifier. Figure 6.



Schematic of circuit for detecting phase difference between polarographic and reference signal. H, I, J, are Philbrick K2X-A amplifiers. <u>'</u> Figure

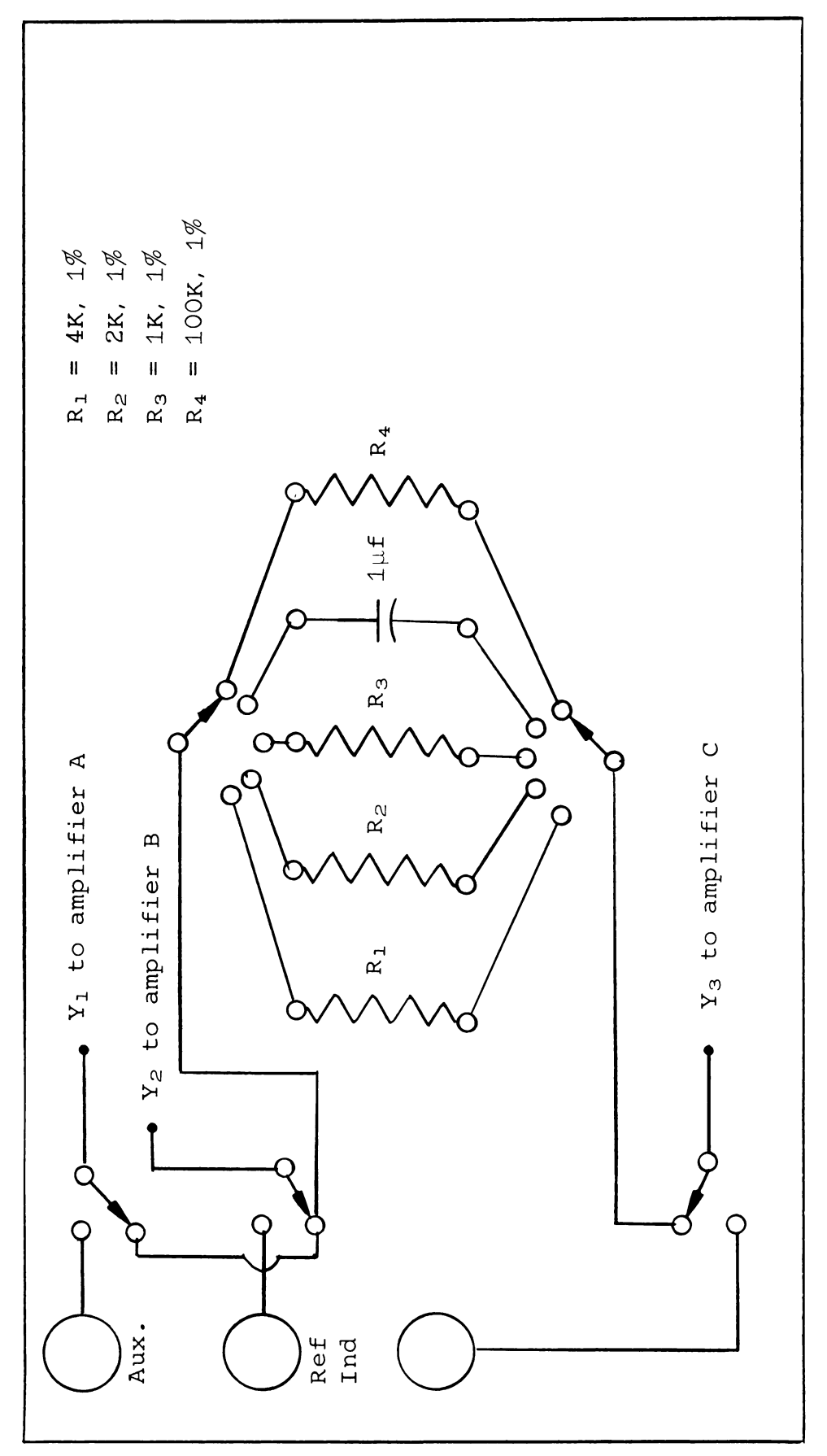
The signal from the tuned amplifier is converted by amplifiers H and I to a constant amplitude square wave. A reference a.c. signal with a known phase relationship to the potential being applied to the cell is also converted by amplifier J to a constant amplitude square wave. The two square waves are then added and rectified. The signal resulting from these operations has a d.c. component dependent on phase relationships between the square waves, this signal being a maximum when the square waves are in phase and zero when they are 180° out of phase.

Amplifiers H and I are in series to insure that even small signal levels from the tuned amplifier are converted to square waves. The rise time of amplifiers H, I, and J is improved by positive feedback via capacitative coupling of the output and the positive input of the operational amplifier. This causes pulsing of the amplifier during the rising portion of the square wave. It is very essential to minimize rounding of the edges of the square wave by small signals at high frequencies otherwise the phase-angle signals vary with amplitude of input signal.

Calibration of D.C. Currents

The d.c. mode (Figure 2) consists of a 100K resistor which makes amplifier D a unity gain inverter.

For current calibration, the electrodes are taken out of the circuit and connection to the precision 100K resistor is made as shown in Figure 8. Since the input of operational



Schematic of potentiostat switched to the calibrating mode. $Y_1,\ Y_2,\ Y_3,\ see\ Figure\ 2.$ Figure 8.

amplifier C is a virtual ground, the potential appearing at amplifier B is placed across the 100K resistor and the current flowing through the resistor is $E_{\rm B}/100{\rm K}$. Since D is a unity gain amplifier, its output potential will be equal to the output of C but of opposite sign.

For d.c. operation the resistance of $R_{\rm L}$ is 100K. To calibrate the recorder response, 0 volt, introduced by the d.c. potential source (Figure 3) is measured to within a millivolt and placed across the 100K resistor. This will define the zero current on the recorder. Then $E_{\rm B}$ measured to within a millivolt is placed across the 100K resistor. This corresponds to a current of $E_{\rm B}/100$ K. The corresponding signal from amplifier D is then attenuated to give a convenient recorder deflection. The ultimate accuracy of the current measured will depend upon the accuracy of the 100K resistor. At this point the electrodes may be switched back into the circuit and a potential-current curve recorded.

Calibration of A.C. Currents

To measure fundamental a.c. signals free from noise, amplifier F (Figure 5) must be tuned sharply to the frequency of the signal to be measured. The proper R_1 value is selected to provide the desired frequency ($f_1 = \frac{1}{2\pi R_1 C}$), R_2 is set equal to R_1 , and R_3 is adjusted until oscillations in amplifier F cease. The frequency of the a.c. source is adjusted until the output of amplifier F is at a maximum. R_1 , R_2 , or R_3 (Figure 8) is selected to provide the desired

current range (I = E_B/R). E_B is measured across R_1 , R_2 or R_3 with the oscilloscope. Amplifier D is adjusted until a convenient deflection on the recorder is attained.

The lower calibration limit should never be zero current. The reason is that diodes are not perfect conductors in the forward direction at low current levels. Therefore the current response of the recorder would not be linear from zero to the upper current limit. The lower current calibration should be $0.5\mu a$ or greater. This is no limitation since capacitative currents in this work were typically 1 to $30\mu a$ depending upon the frequency of the applied a.c. potential.

Phase-Angle Calibration

With amplifier F (Figure 5) tuned to the desired frequency, the phase-angle detector is switched in as shown in Figure 7. With the calibrating circuit switched to the $1\mu f$ capacitor, the phase-shifter (Figure 7) is adjusted until the recorder gives nearly a zero reading. The bucking potential (Figure 6) is adjusted until the recorder gives a zero reading. The calibrating circuit is then switched to a resistor, R_1 , R_2 , or R_3 , and amplifier D is attenuated to a convenient recorder setting. Since the a.c. signal through the $1\mu f$ capacitor leads the applied a.c. potential by 90° , the lower limit setting represents a signal 90° out of phase. Since the a.c. signal through a resistor is in phase with the applied potential, the upper limit represents a 0°

phase-shift. The long term stability of the employed commercial oscillator was about 0.5°, therefore the above calibration was performed before and after each phase-angle measurement.

The accuracy of the phase-angle detector was tested with the following series RC networks (components of 1% accuracy): 500 ohm and 1.0 μ f; 100 ohm and 1.0 μ f; 50 ohm and 1.0 μ f. The phase-angles measured agreed to within 1% of the calculated values throughout the 30 to 1100cps frequency range. These RC circuits and frequencies yielded the current range from 0.93 μ a to 33 μ a and the phase-angle range from 89.6° to 17.6°.

Other Equipment

The electrolysis cell employed in this work is shown in Figure 9. Through the side-arm with the two-way stop cock, nitrogen can either be bubbled through the solution by way of a coarse frit at the bottom of the cell or blown over the top of the solution. The cell is fitted with a 3-hole rubber stopper through which the electrodes (dropping mercury electrode, saturated calomel electrode, and the auxiliary electrode) are introduced.

The constructional details of the reference electrode employed are shown in Figure 10. The reference electrode was separated from the polarographic solution by an isolation compartment which usually contained the supporting electrolyte. Both the reference electrode and the isolation

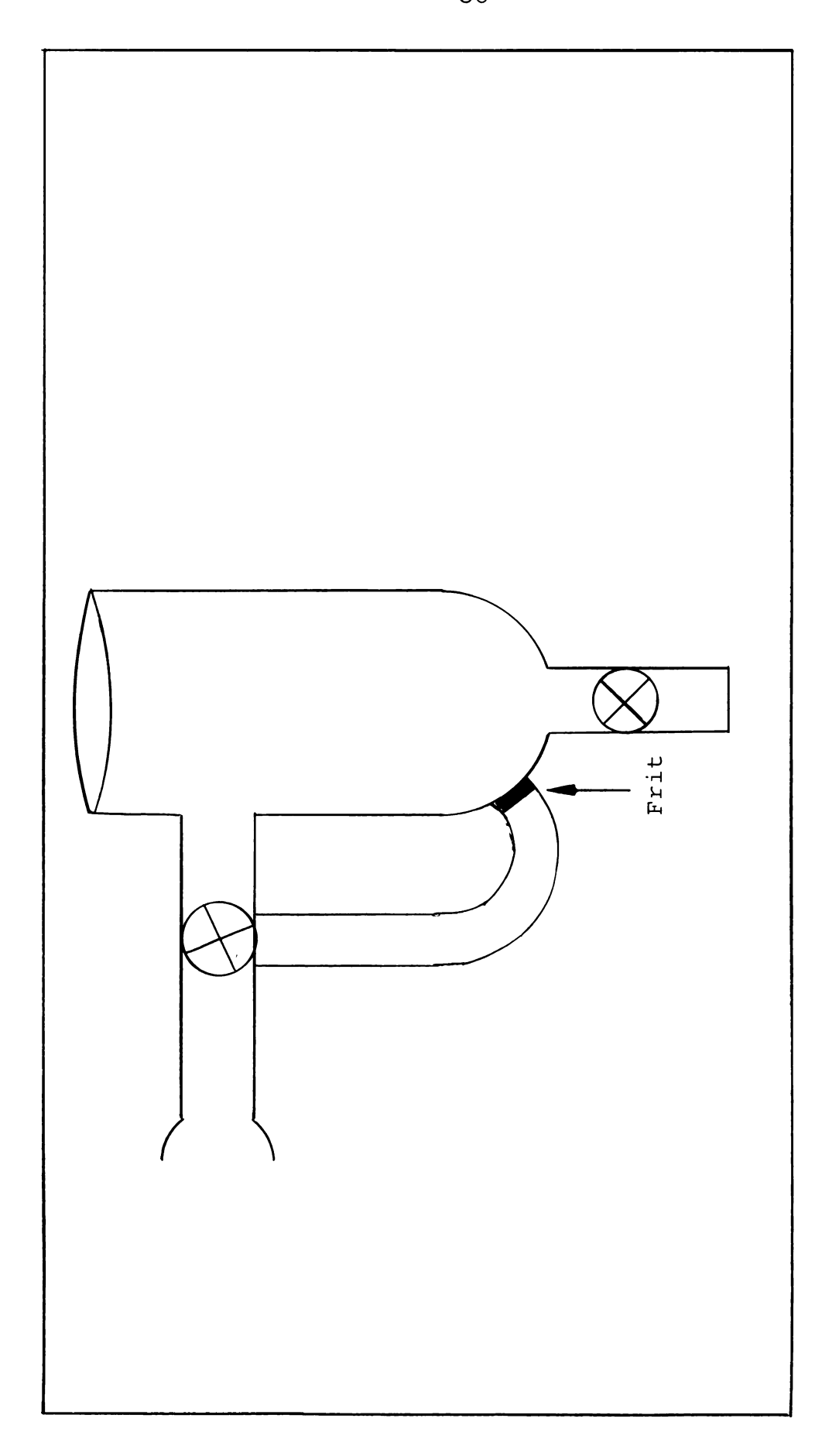


Figure 9. Electrolysis Cell.

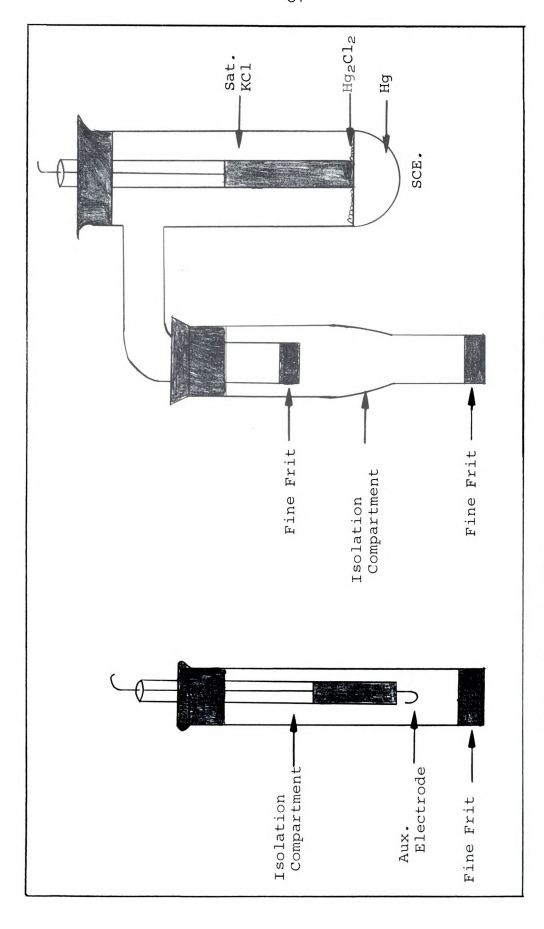


Figure 10. Auxiliary and reference electrode.

compartment were tightly stoppered to minimize any flow of solution through the frits. Isolating the reference electrode minimizes contamination of the polarographic solution by foreign ions from the side arm of the reference electrode.

The auxiliary electrode, a platinum wire, is separated from the polarographic solution by a fine frit. Its isolation compartment always contained the polarographic solution.

The frit prevented the free diffusion of oxidation products to the dropping mercury electrode.

Reagents

Mercury

Reagents were employed without further purification.

The chemicals, and sources are as follows:

The enemicals, and bouldes are a	15 10110W3.
Cadmium Nitrate Tetrahydrate	Baker's Analyzed Reagent
Potassium Chloride	Matheson, Coleman and Bell. A.C.S. Reagent
Sodium Chloride	Baker's Analyzed Reagent
Perchloric Acid	Baker's Analyzed Reagent
Disodium Salt of Ethylenedi-	Mallenckrodt Analytical
aminetetraacetic Acid (EDTA)	Reagent
Sodium Sulfate	Baker's Analyzed Reagent
Hydrochloric Acid	Baker's Analyzed Reagent
Sulfuric Acid	Baker's Analyzed Reagent
Sodium Perchlorate Monohydrate	G. Frederick Smith
	Chemical Company
Potassium Nitrate	Matheson, Coleman, and Bell A.C.S. Reagent Grade
Nitrogen	Prepurified, 99.996% The Matheson Company

Purified in this laboratory

Preparation of Solutions

A 0.0100M Cd(II) stock solution was prepared from $Cd(NO_3)_2 \cdot 4H_2O$ and standardized by EDTA titration (36).

The supporting electrolyte solutions were prepared by weighing solids or pipeting liquid electrolytes and diluting to volume.

The sample solution was prepared by appropriate dilution of cadmium stock aliquots to which the desired amount of electrolyte had been added.

None of the solutions contained maximum suppressor.

All solutions were prepared from the laboratory distilled water supply. These solutions yielded no different results than when triply distilled water was used.

Dissolved oxygen was removed from all solutions in the electrolysis cell by bubbling with nitrogen for a period of 20 minutes. Last traces of oxygen were removed from the nitrogen by bubbling it through an acid vanadous sulfate solution, dilute NaOH, and $\rm H_2O$ before passing it into the electrolysis cell.

All polarograms were run at $24 \pm 1^{\circ}$.

Evaluation of E_1 , E_1 , E_3 from D.C. Polarograms

The current-potential values for the sample solution were determined manually every 10mv from the foot of the wave to well into the limiting current region. In the same potential region the current-potential relationship was determined for the supporting electrolyte. The current of

the sample solution was corrected for the residual current. The values of $E_{\frac{1}{4}}$, $E_{\frac{1}{2}}$, $E_{\frac{3}{4}}$, were determined by the log equal to 0.477, 0, -0.491 intercepts of a $E_{\text{d.c.}}$ versus log i_{d} -i/i plot.

Evaluation of D_O and D

 D_0 , the diffusion coefficient of the oxidized species was calculated with the aid of the Lingane-Loveridge equation (27). The parameters necessary for this evaluation are i_d (average diffusion current), C (millimole concentration of electroactive species), m (mg/sec of mercury delivered by the electrode), t (drop time).

To obtain average diffusion currents, the maximum diffusion current was multiplied by 6/7. The capillary characteristics (m and t) were evaluated at the potential at which the diffusion current was measured. The drop time, (t), was evaluated by timing the fall of 20 drops and m from the weight of the 20 drops and known t.

The evaluation of D was accomplished with the aid of equation 17 and using the value of D $_{\rm R}$ equal to 1.61 x 10⁻⁵ cm²/sec obtained by Bauer and Elving (5).

Evaluation of Cd. l. and Rt

The determination of the capacity of the double-layer $(C_{\text{d.l.}})$ and total resistance (R_{t}) is accomplished by applying a 5mv a.c. potential of a known frequency to the cell containing supporting electrolyte, and measuring the amplitude of the resulting a.c. current and its phase-angle.

Since the capacity of the double-layer changes with d.c. potential and electrode area, current and phase-angles are determined at maximum drop size at each d.c. potential of interest.

The capacity of the double-layer is calculated by

$$C_{d.l.} = \frac{\Delta I}{\omega \Delta E \sin \Phi}$$
 (32)

and total series resistance by

$$R_{t} = \frac{\Delta E}{\Delta I} \cos \Phi \tag{33}$$

The evaluation of $C_{\rm d.l.}$ and $R_{\rm t}$ was determined at least at two different frequencies. It was found that the values obtained were independent of frequency within experimental error. However, since the value of $\cos \phi$ changes rapidly at phase-angles greater than 88° , these experiments were performed at 300 and 550 cps to obtain smaller phase-angles.

Evaluation of α and k_h

By performing three experiments, the mass transfer coefficient (α), the heterogeneous rate constant uncorrected for activities (k_h), and mechanism of the electrode process can be determined by measuring the following:

- (1) The phase-angle dependence on potential at low frequency (~30cps).
- (2) The phase-angle dependence on potential at high frequency (~820cps).

(3) The phase-angle dependence on frequency at d.c. potentials corresponding to $E_{\frac{1}{4}}$, $E_{\frac{1}{2}}$, $E_{\frac{3}{4}}$.

The experiments were performed with an a.c. potential of 5mv. All phase-angles were corrected for double-layer and total series resistance effects with a Control Data 3600 computer.

The mass transfer coefficients were calculated by equation (22) and equation (23).

Equation (22) depends upon the location of the d.c. potential where cot ϕ is a maximum. This is best accomplished by employing the high frequency data of experiment 2, since in these experiments cot ϕ has larger values, and the effect of chemical reaction on cot ϕ are negligible.

Equation (23) depends upon determining the slope (equation (19)) from the phase-angle dependence on frequency (equation (18)) at two different d.c. potentials.

The heterogeneous rate constant, k_h , can be readily calculated with the aid of equation (21) and (17), once the slope from cot ϕ versus $\omega^{\frac{1}{2}}$ plot (equation (18)) has been evaluated at a d.c. potential corresponding to $E_{\frac{1}{2}}^R$.

Once the parameters k_h , α , β , D are evaluated, they are introduced into equation 18, and a phase-angle dependence on d.c. potential is calculated at the low frequency employed. The calculated plot is then compared to the experimental one in order to determine if the mechanism involves just diffusion and charge-transfer or some other rate controlling steps.

DISCUSSION OF RESULTS

Evaluation of E_1 , E_1^R , E_3 and D_0

Values of the experimental half-wave potential, $E_{\frac{1}{2}}^{R}$, and the calculated diffusion coefficient, D_{0} , of the oxidized species for the various supporting electrolytes, as well as quantities needed to calculate D_{0} , are tabulated in Table I.

Shifts of $E_{\frac{1}{2}}^R$ to more negative potentials usually indicate complexation of the reducible species, the more stable the complex, the more negative $E_{\frac{1}{2}}^R$.

On the basis of this expected behavior, the $E_{\frac{1}{2}}^{R}$ values indicate that the relative strengths of the complexes formed between Cd(II) and the anions of the supporting electrolyte follow the order:

$$C1^{-} > SO_{4}^{-} > NO_{3}^{-} > C1O_{4}^{-}$$
.

This is not the exact order which would be expected from published values (7) of the log of the formation constants which for Cd(II) and the anions in the order listed above are respectively:

This is an indication that other factors affecting $E_{\frac{1}{2}}^R$ shifts must also be considered. One of these could be junction potentials which exist at boundaries between dissimilar electrolytes.

This becomes obvious when the $E_{\frac{1}{2}}^R$ value for 1M NaClO₄ is compared to the one for 1M HClO₄. In both experiments the

 E_{2}^{R} , i_d and D_o Values for 1.0mM Cd(II) in Various Supporting Electrolytes Table I.

Supporting Electrolyte	ER a vš. SCE, v	Av. id, µa	Slope	$D_0 \times 10^6$, cm^2/sec	t, sec	m, mg/sec
0.5M Na ₂ SO ₄	-0.604	5.31	0.0296	4.52	5.40	1.676
$1M \text{ Na}_2 \text{SO}_4$	909.0-	4.87	0.0292	3.93	5.42	1.666
0.5M Na ₂ SO ₄	-0.594	5.98	0.0296	5.70	5.34	1.684
1M H ₂ SO ₄	-0.597	5.81	0.0295	6.41	5.39	1.678
$1M \text{ KNO}_3$	-0.585	6.40	0.0293	6.46	5.38	1.676
1M HClO ₄	-0.607	6.54	0.0296	6.67	5.32	1.687
1M NaClO4	-0.573	6.33	0.0293	6.45	4.99	1.686
1M KCl	-0.642	6.85	0.0295	7.30	5.39	1.678
1M HCl	-0.644	69.9	0.0294	6.70	5.41	1.673
1M NaCl	-0.635	6.59	0.0298	6.82	5.42	1.673

 $^{\rm a}{
m Determined}$ at the log = 0 intercept from the plot by log

 $b_{\Delta E/\Delta} \log \frac{id-i}{i} = \frac{0.059}{n}$

^cat - 0.750 v vs. SCE

reference electrode was separated from the sample solution by an isolation compartment containing 1M NaNO3 instead of 1M HClO4 to prevent the precipitation of KClO4 at the SCE arm. That the $E_{\frac{1}{2}}^R$ values are dependent on the concentration and type of electrolyte in the isolation compartment is shown in Table II. This dependence must be due to a junction potential arising from the difference of diffusion rates of ions through both junctions, that is, saturated KCl/isolation electrolyte, isolation electrolyte/1M HClO4. On changing the isolation electrolyte from 1M NaNO3 to 0.1M NaNO3, $E_{\frac{1}{2}}^R$ shifted to a more negative potential, and when changed to 1M HNO3 shifted it to a more positive potential.

A point of interest is that the value of the slope, from the plot of $\log i_{\rm q}$ -i/i versus $E_{\rm d.c.}$ plot (Tables I and II), is independent of the concentration and type of electrolyte in the isolation compartment. The current-potential curves retain their expected shape and only their relative position compared to the reference electrode is shifted.

 $\rm E_{\frac{1}{4}}$ and $\rm E_{\frac{3}{4}}$ values were determined from the intercepts at log equal to 0.477 and -0.491 respectively on a log $\rm i_d$ -i/i versus $\rm E_{d.c.}$ plot. $\rm E_{\frac{1}{4}}$ and $\rm E_{\frac{3}{4}}$ were displaced 14mv from $\rm E_{\frac{1}{4}}$ in all media.

Typical A.C. Polarograms

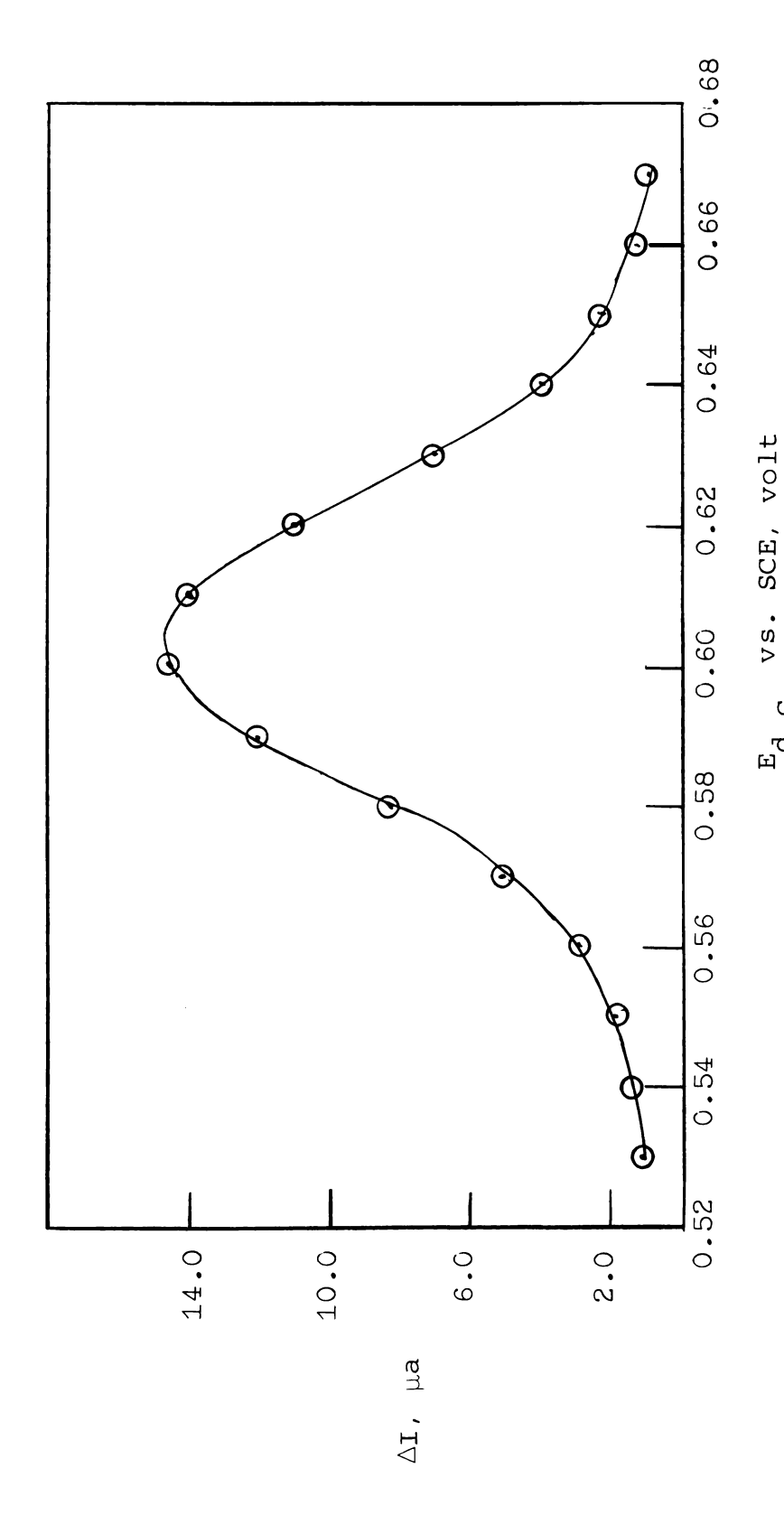
Figures 11 and 12 illustrate typical total fundamental-harmonic a.c. polarograms of 1.0mM Cd(II) in 1M Na $_2$ SO $_4$ at

Table II. Variation of E_1^R with Concentration and Type of Electrolyte in Isolation Compartment. Sample Solution is 1.0mM Cd(II) in 1M HClO₄

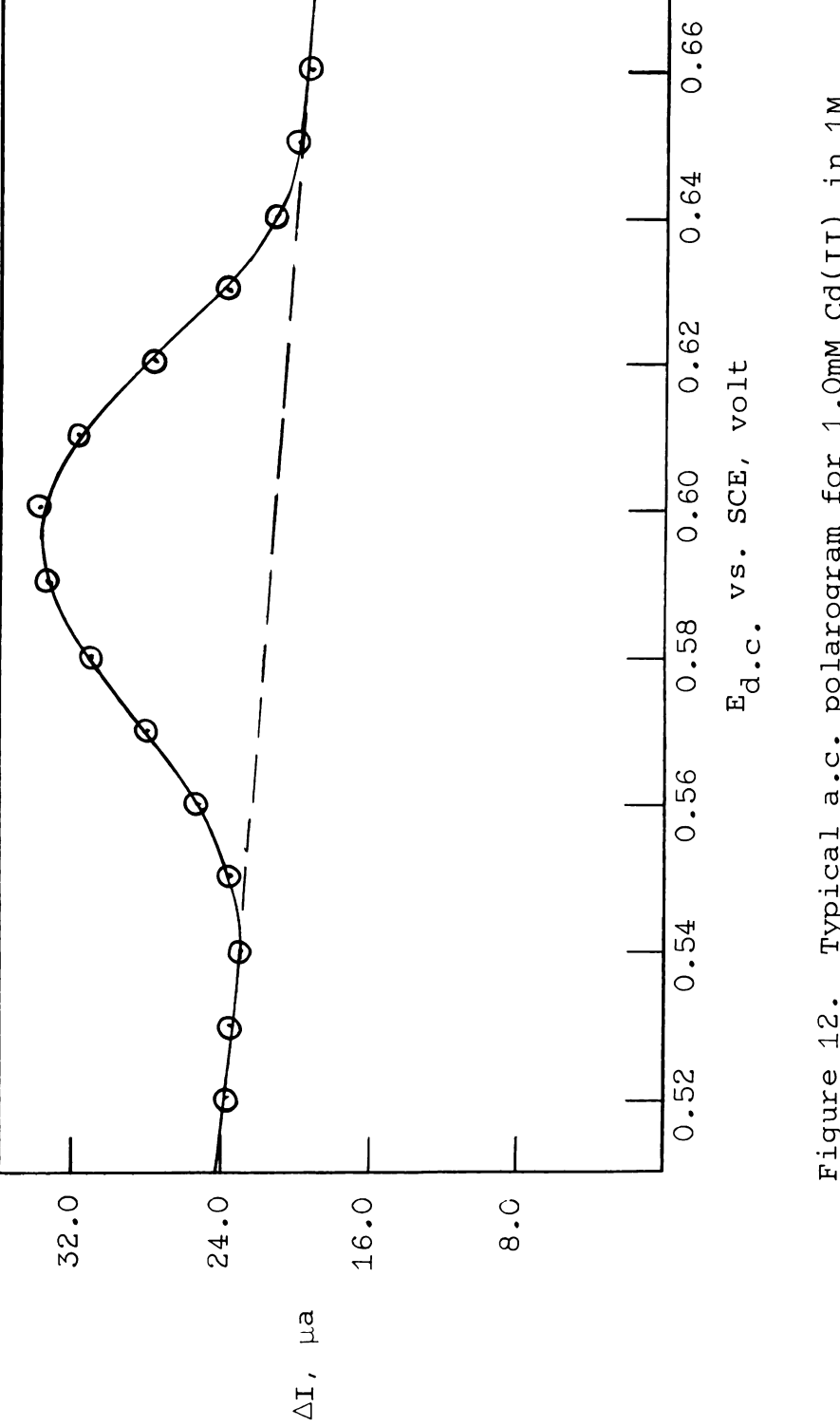
Isolation Compartment	El vs. sce, v	Slope b
1M NaNO ₃	-O.607	0.0296
0.1M NaNO ₃	-0.646	0.0294
1M HNO ₃	-0.586	0.0294

^aDetermined at the log = 0 intercept from the plot log i_d-i/i vs. $E_{d.c.}$.

 $^{^{}b}\Delta E/(\Delta \log i_{d}-i/i) = \frac{0.059}{2}$



Typical a.c. polarogram for 1.0mM Cd(II) in 1M $\mathrm{Na}_2\mathrm{SO}_4$ at 33.8cps. Figure 11.



Typical a.c. polarogram for 1.0mM Cd(II) in 1M Na $_2 SO_4$ at 822cps. Figure 12.

33.8 and 822cps respectively. It is evident from Figure 12 that from the base-line level, the total alternating current is made up largely of capacitative current at high frequencies.

Table III compares the measured phase-angle with the corrected (faradaic) phase-angle. It becomes apparent that the correction becomes greater as the faradaic current becomes small compared to the capacitative current.

Evaluation of Transfer Coefficient, α

The values of the transfer coefficient, α , obtained from the ratio of slopes $(\frac{\Delta \cot \phi}{\Delta \omega \frac{1}{2}})$ at two different d.c. potentials are tabulated in Table IV. Transfer coefficients of Cd(II) in the chloride and the nitrate media were not calculated in this manner since the ratio of the uncertainties in the slopes became competitive with the values of the ratio of the slopes.

Transfer coefficients were also calculated from the d.c. potential (equation (22)) where $\cot \Phi$ is a maximum. Table V compares the values of the transfer coefficients calculated by equation (22) and (23).

Both methods for calculating the mass transfer coefficients give comparable values as long as the charge-transfer rate is sufficiently slow (0.3cm/sec > k_h' > 10^{-4} cm/sec). As the charge-transfer rate becomes larger, the evaluation of α becomes more uncertain by either method. However, even for large charge-transfer rates (k_h' \cong 1cm/sec)

Table III. Variation of Cd.1. and Phase-Angle Correction with Changing Ed.c. for 1.0mM Cd(II) in 1M $_{\rm Na_2SO_4}$ at 822cps

				
(E vs. SCE),	ν ΔΙ μα	c _{d.1.} ,μf	Φ'Measured (degrees)	φ corrected ^{a,b} (degrees)
0.55	23.50	0.903	59.9	36.7
0.56	25.45	0.891	52.3	39.8
0.57	27.90	0.880	41.5	35.0
0.58	31.15	0.865	31.0	30.7
0.59	33.45	0.853	23.5	25.2
0.60	33.80	0.840	20.0	20.3
0.61	31.60	0.826	21.3	17.7
0.62	27.65	0.815	27.3	16.4
0.63	23.70	0.806	38.1	17.4
0.64	21.10	0.793	49.6	18.5
0.65	19.85	0.782	59.5	19.2

 $^{^{\}rm a}$ Corrected for $^{\rm C}$ d.l. and $^{\rm R}$ t by equation (31).

 $b_{R_t} = 77.2 \text{ ohms.}$

The second secon		

Table IV. Values of the Transfer Coefficient, α , Obtained from Slope Measurements for 1.0mM Cd(II) in Various Supporting Electrolytes

Supporting Electrolyte	Slope ^a at	Slope ^a at	Slope ^a at E ₃	α ^b
0.5M Na ₂ SO ₄	1.42×10^{-2}	2 2.26 x 10 ⁻²	2.72 x 10 ⁻²	0.20 <u>+</u> 0.03
1M Na ₂ SO ₄	1.67 x 10-2	² 2.63 x 10 ⁻²	3.05 x 10 ⁻²	0.22 ± 0.03
0.5M H ₂ SO ₄	0.911x 10 ⁻²	² 1.42 x 10 ⁻²	1.58 x 10 ⁻²	0.24 <u>+</u> 0.03
1M H ₂ SO ₄	1.01 x 10 ⁻²	² 1.57 x 10 ⁻²	² 1.77 x 10 ⁻²	0.25 ± 0.03
1M HClO ₄	5.78×10^{-3}	8.33 x 10 ⁻³	9.11 x 10 ⁻³	0.30 ± 0.04
1M NaClO ₄	4.11 × 10 ⁻³	3 6.11 x 10 ⁻³	3 6.55 x 10 ⁻³	0.28 ± 0.04

^aDetermined from $\frac{\triangle \cot \Phi}{\triangle \omega \frac{1}{2}}$ at a constant d.c. potential

bottained from ratio of slopes $E_{\frac{1}{4}}/E_{\frac{1}{2}}$, and $E_{\frac{1}{2}}/E_{\frac{3}{4}}$, see equation (23).

Table V. Values of the Transfer Coefficient, α , for 1.0mM Cd(II) in Various Supporting Electrolytes

Supporting Electrolyte	$(E_{d.c.}^{R}-E_{\frac{1}{2}}^{R})$, mv	α b	α ^c
0.5M Na ₂ SO ₄	16.5	0.21 ± 0.03	0.20 ± 0.03
1M Na ₂ SO ₄	17.5	0.20 ± 0.03	0.20 ± 0.03
0.5M H ₂ SO ₄	12.5	0.27 ± 0.03	0.24 ± 0.03
1M H ₂ SO ₄	14.5	0.24 ± 0.03	0.25 ± 0.03
1M KNO ₃	0.0	0.50± 0.05	
1M HClO ₄	13.5	0.26 ± 0.04	0.30 ± 0.04
1M NaClO ₄	10.0	0.31 ± 0.04	0.28 ± 0.04
1M KCl	3.0	0.44 ± 0.05	
1M HCl	4.0	0.42 ± 0.05	
1M NaCl	2.0	0.46 ± 0.05	

 $^{^{\}rm a}$ Potential at which cot $^{\rm \phi}$ is maximum

 $^{^{\}mathrm{b}}$ Calculated when cot $^{\mathrm{o}}$ was maximum by equation (22).

Average value determined from $\frac{\Delta \cot \Phi}{\Delta \omega \frac{1}{2}}$ at two different d.c. potentials, see equation (23).

the location of the d.c. potential where cot ϕ is a maximum can be determined to within \pm 3mv.

Evaluation of the Heterogeneous Rate Constant, kh

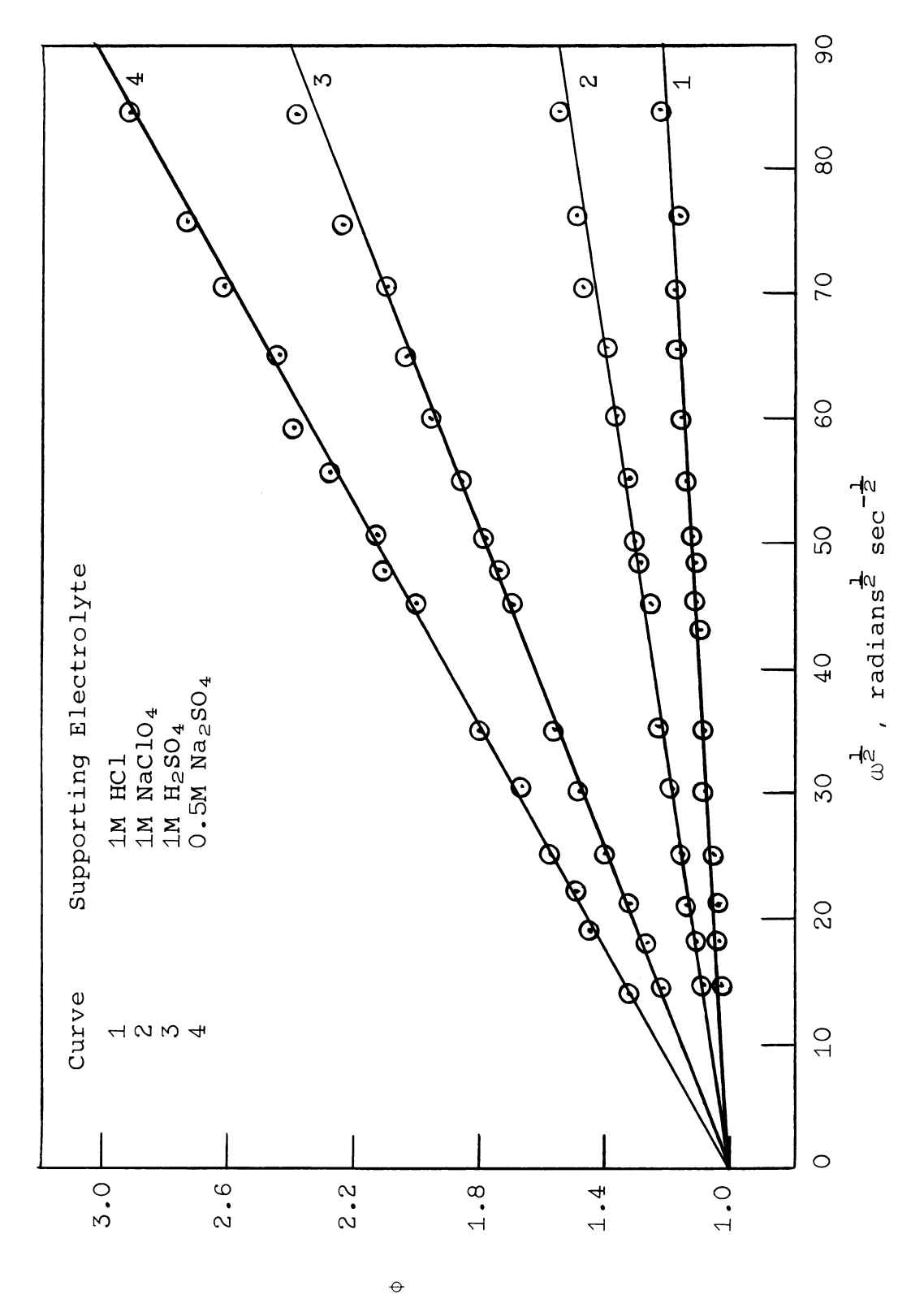
Typical plots of cot ϕ versus $\omega^{\frac{1}{2}}$ at $E_{\text{d.c.}} = E_{\frac{1}{2}}^{R}$ are illustrated in Figure 13 for 1.0 mM Cd(II) in various supporting electrolytes. All of the plots yield straight lines up to frequencies of about 1100cps with intercepts at cot ϕ = 1, extrapolated to zero frequency, which is expected for the following reversible electrode process

$$0 + ne \longrightarrow R$$
.

Such linearity was not attained by previous investigators (3, 4, 5).

Table VI lists the slope $(\frac{\Delta \cot \Phi}{\Delta \omega \frac{1}{2}})$ at $E_{d.c.} = E_{\frac{1}{2}}^{R}$, D, and the values of the heterogeneous rate constants uncorrected for activity coefficients for 1.0mM Cd(II) in various supporting media. The values of the heterogeneous rate constant, k_h , ranged from 0.063cm/sec in 1M Na₂SO₄ to 1.2cm/sec in both 1M NaCl and 1M KCl.

The effect of Cd(II) concentration on the k_h^{\dagger} is shown in Table VII to be constant within experimental error. The larger deviation of k_h^{\dagger} in 1M Na₂SO₄ is caused by the larger error in the corrected phase-angle. The problem arises any time the faradaic current becomes small compared to the total current. For 0.2mM Cd(II) the faradaic current is equal to the capacitive current at 33cps and is about 10%



cot

Variation of cot Φ with changing a.c. frequency for 1mM Cd(II) in various supporting electrolytes. Figure 13.

Table VI. Values for the Heterogeneous Rate Constant, k_h , for 1.0mM Cd(II) in Various Supporting Electrolytes. Values for Cd.1. and Rt, for Electrode Used are Included.

Supporting Electrolyte	Slope ^a $\frac{\Delta \cot \Phi}{\Delta \omega_2^4} \times 10^2$	Dx10 ⁶ , cm ² /sec	Cd.l., c	R _t , ohms	k', cm/sec
0.5M Na ₂ SO ₄	2.26	5.89	0.816	87.3	0.076
1M Na ₂ SO ₄	2.63	5.51	0.833	77.2	0.063
0.5M H ₂ SO ₄	1.42	7.54	0.857	64.4	0.14
1M H ₂ SO ₄	1.57	7.03	0.952	58.9	0.12
1M KNO ₃	0.358	10.20	1.14	76.4	0.63
1M HClO ₄	0.833	8.38	1.09	60.6	0.25
1M NaClO ₄	0.611	8.57	1.11	81.3	0.34
1M KCl	0.189	10.34	1.11	72.6	1.2
1M KCl	0.233	9.68	1.12	60.2	0.94
1M NaCl	0.189	10.36	1.08	78.0	1.2

^aAt $E_{\frac{1}{2}}^{R}$ ^bD = Do $^{\beta}$ D_R $^{\alpha}$

Cat $E_{d.c.} = E_{\frac{1}{2}}^{R}$ vs. SCE.

Table VII. Effect of Cd(II) Concentration on the Heterogeneous Rate Constant, \mathbf{k}_{h}

Supporting Electrolyte	Conc. Cd(II),mM	Slope, a $\frac{\triangle \cot \phi}{\triangle \omega} \times 10^2$	k' _h , cm/sec
1M Na ₂ SO ₄	1.0	2.63	0.063
1M Na ₂ SO ₄	0.2	2.28	0.073
1M H ₂ SO ₄	1.0	1.57	0.12
1M H ₂ SO ₄	2.0	1.64	0.11
1M KNO ₃	1.0	0.358	0.63
1M KNO ₃	2.0	0.376	0.60

^aAt $E_{\frac{1}{2}}^{R}$

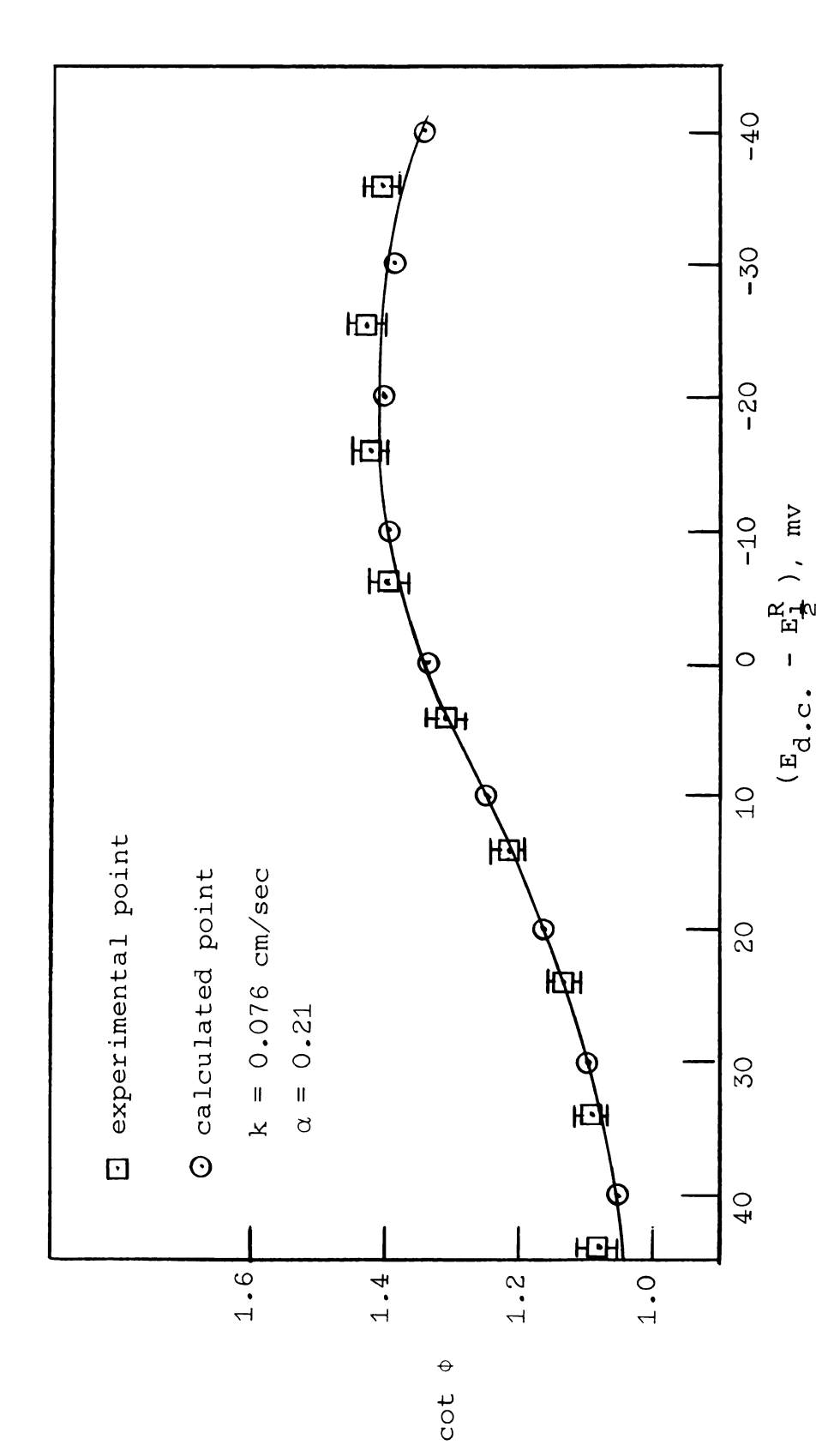
of the total alternating current at 822cps. There is better agreement of $k_h^{'}$ with varying concentrations of Cd(II) in both $\rm H_2SO_4$ and $\rm KNO_3$ pointing out the desirability of working in a concentration range which produces a faradaic current at least one-half the magnitude of the total alternating current measured.

Figures 14, 15, 16, 17 illustrate the comparison between calculated and experimental variation of cot ϕ with changing d.c. potential at low and high frequency for 1.0mM Cd(II) in 0.5M Na₂SO₄ and 0.5M H₂SO₄.

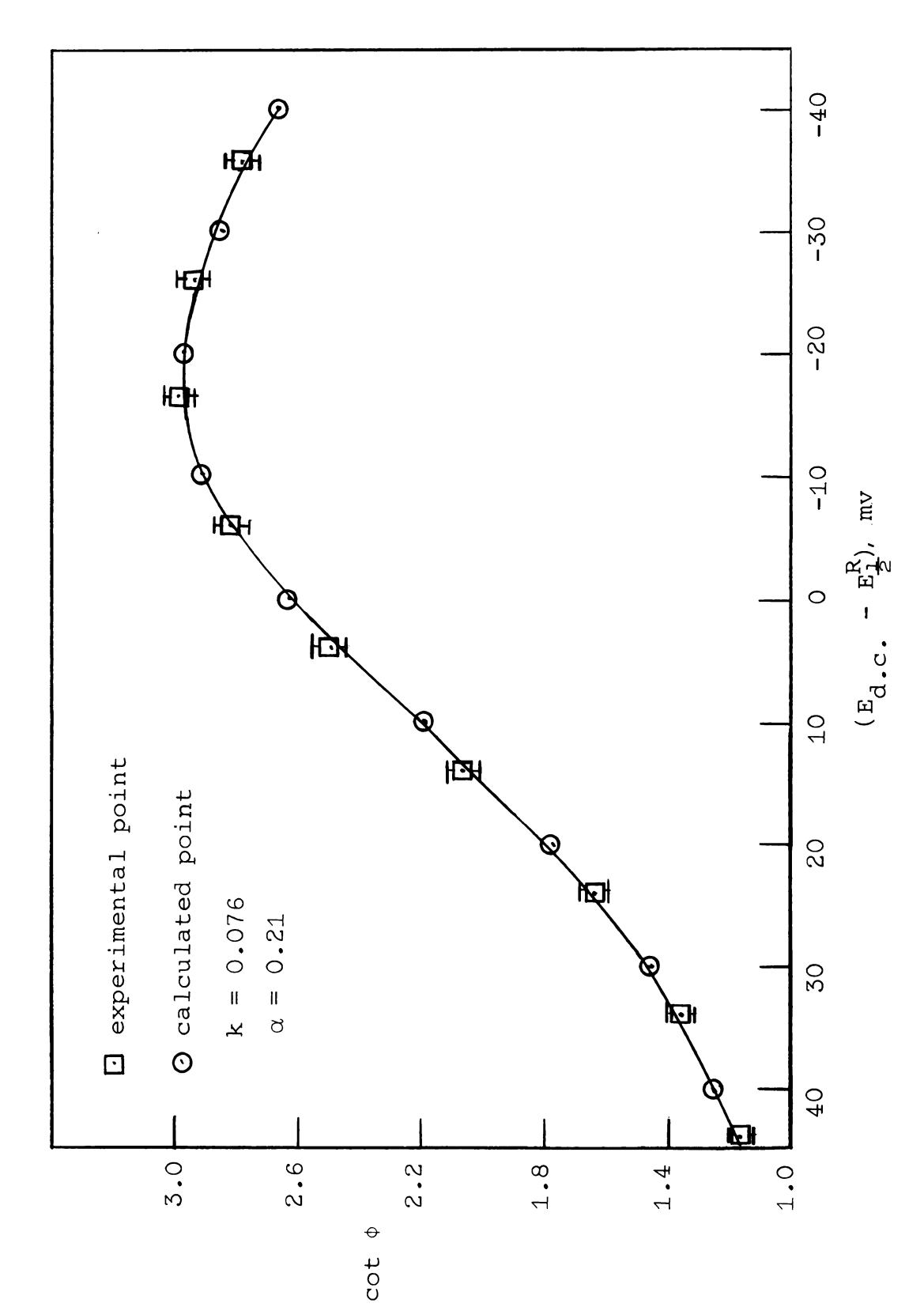
The data (k_h', α, D) in Table VI were used to calculate the theoretical plot for 1mM Cd(II) in all the supporting media with the aid of equation (18). In each case, the experimental cot ϕ , at high or low frequency at various d.c. potentials, agreed well with the calculated cot ϕ . If a maximum uncertainty of \pm 0.5 $^{\circ}$ in the corrected experimental phase-angle values was assumed, each cot ϕ value would vary by the amounts indicated by the vertical line drawn at each experimental point.

The low frequency plots further substantiate that the reduction of Cd(II) in the sulfate and perchlorate media is a simple quasi-reversible electrode process

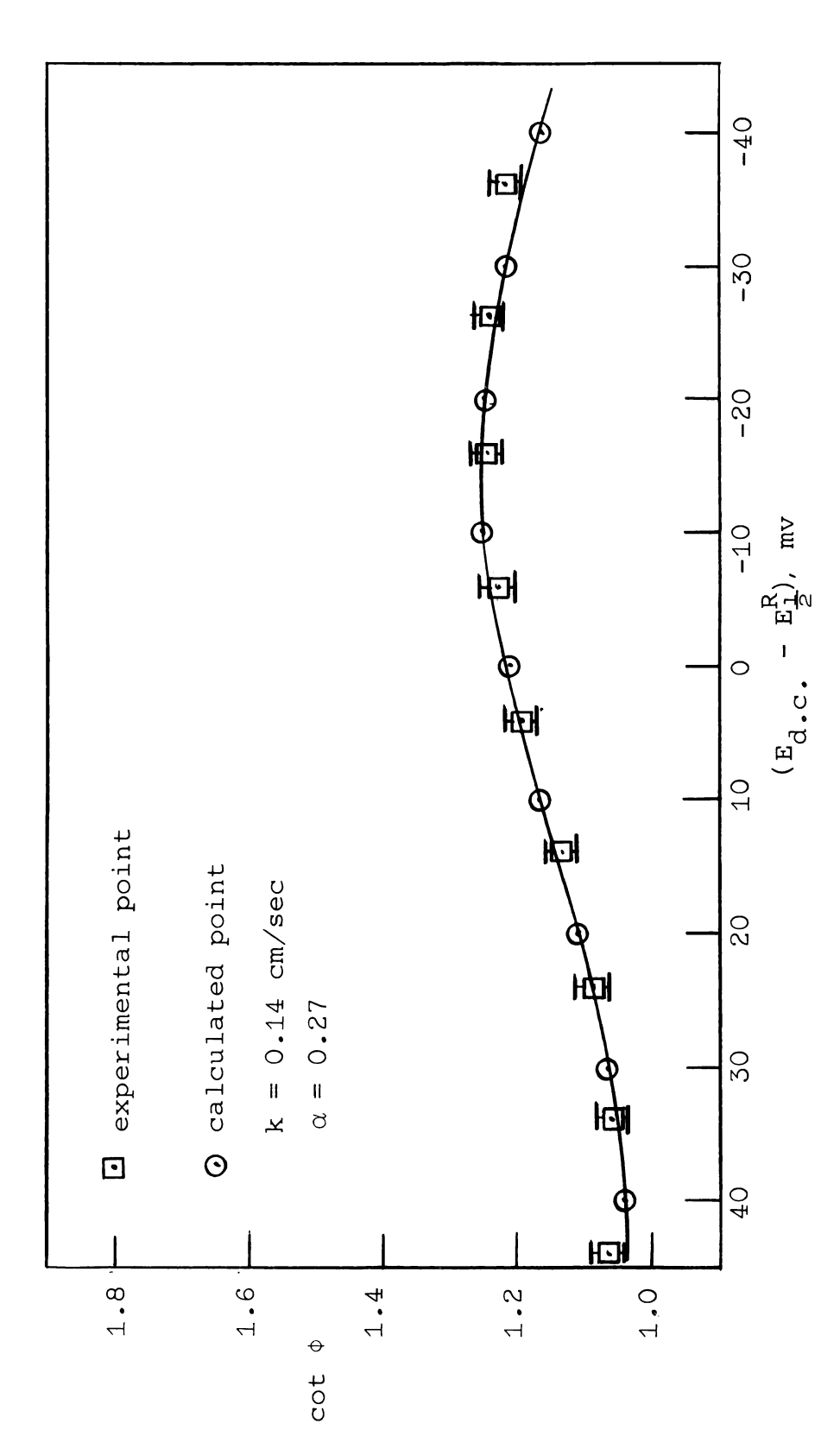
The low frequency data for the nitrate and chloride media neither support nor disprove the above electrode



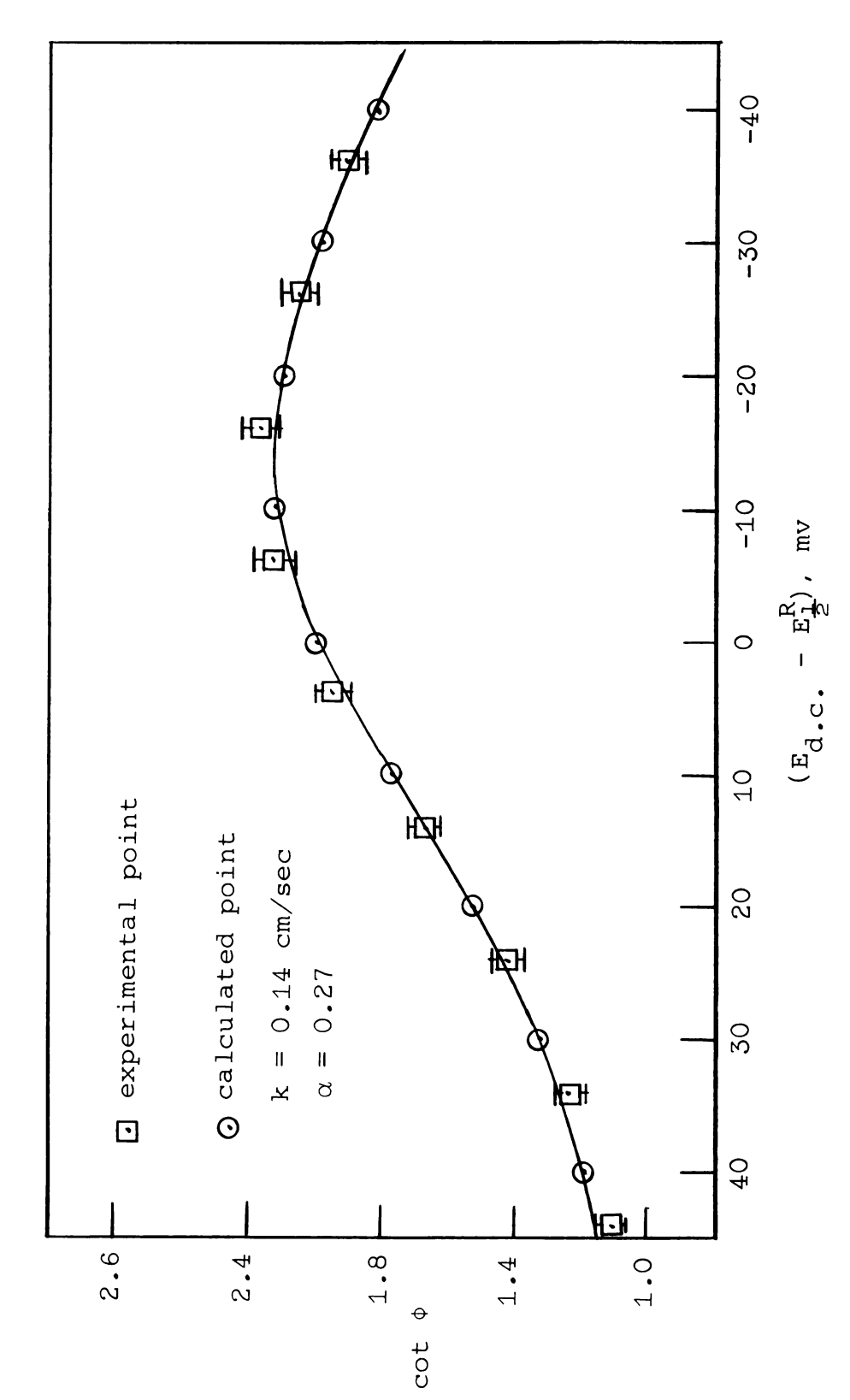
Variation of cot Φ with changing $E_{d,\,C}$ at 34.8cps for 1mM Cd(II) in 0.5M Na_SO_4. Uncertainties of \pm 0.5° indicated on experiin 0.5M Na₂SO₄. mental points. Figure 14.



Variation of cot Φ with changing Eq.c. at 825cps for 1.0mM Cd(II) in 0.5M Na $_2$ SO4. Uncertainties of \pm 0.5 indicated on experimental points. Figure 15.



Variation of cot Φ with changing Eq.c. at 34.4cps for 1.0mM Cd(II) in 0.5M $\rm H_2SO_4$. Uncertainties of \pm 0.5° indicated on experimental points. Figure 16.



Variation of cot Φ with changing Eq.c. at 828cps for 1mM Cd(II) in 0.5M $\rm H_2SO_4$. Uncertainties of \pm 0.5 indicated on experimental points. Figure 17.

process, since the charge-transfer rates are so rapid in these media, that the electrode process becomes dependent on diffusion only and the detection of other kinetic processes becomes impossible. For k_h^i values between 0.6 and 1.2 cm/sec the value of the phase-angle at 33cps for these media should lie between 44 and 45° (45° indicates that the electrode process is only diffusion controlled), and the experimental values agreed typically to within 0.2° of the calculated value.

Table VIII lists the values of k_h and α obtained by other investigators employing various techniques. The reason for the disagreement with some of the investigators is not clear. In general, one can find values of the relative rates of charge-transfer for the reduction of Cd(II) determined by various investigators which are in agreement with our observations, that is, rates decrease in the order, expressed in terms of the anions of the supporting electrolyte,

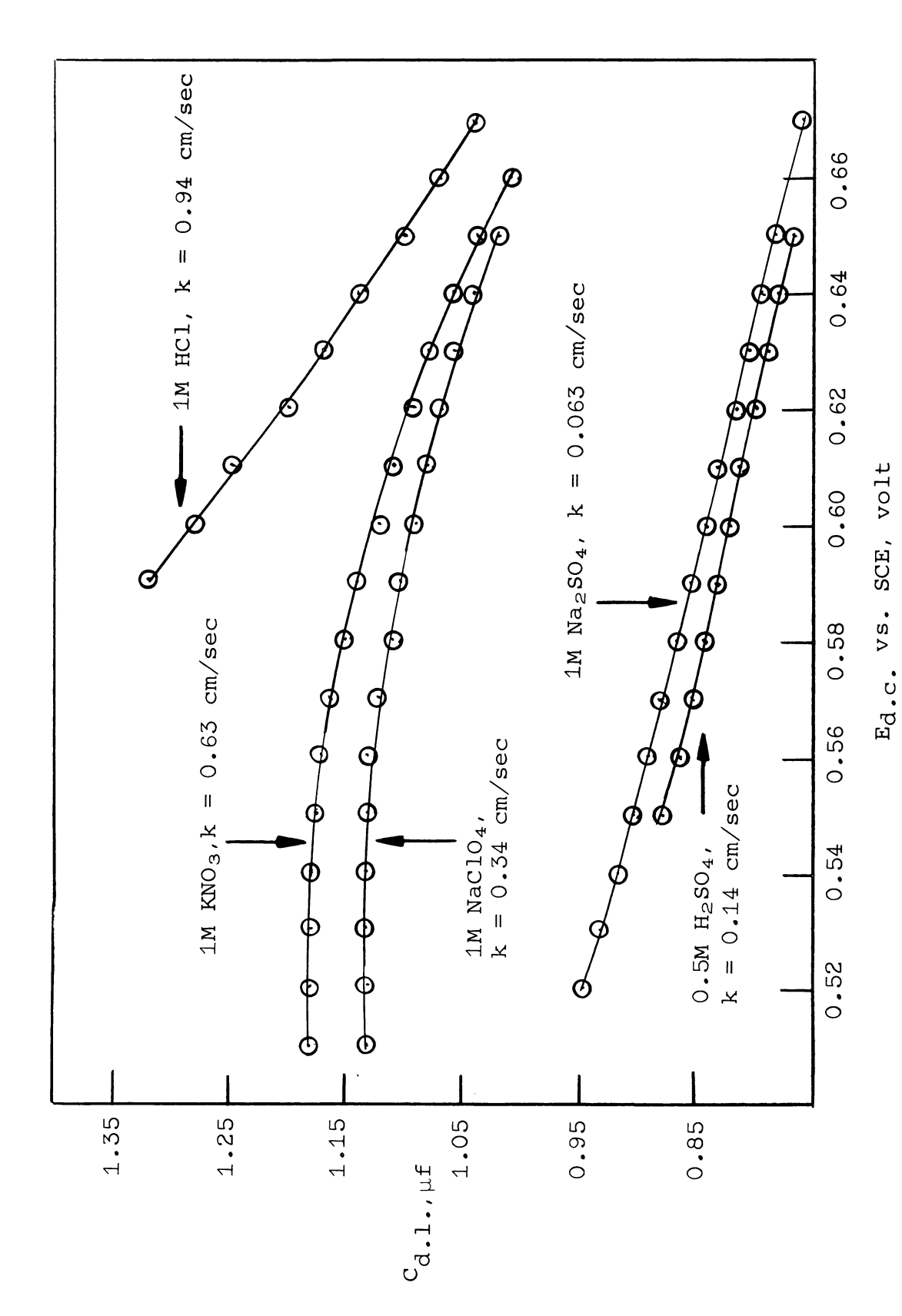
$$C1^{-} > NO_{3}^{-} > C10_{4}^{-} > SO_{4}^{-}$$
.

Because of the heterogeneous nature of electrode processes, it is not too surprising that changes in the double-layer structure or electrode surface would affect the charge-transfer rate. An interesting correlation between the capacity of the double-layer and the charge-transfer rate is illustrated in Figures 18 and 19, that is, the higher the capacity of the double-layer, the more rapid the charge-transfer.

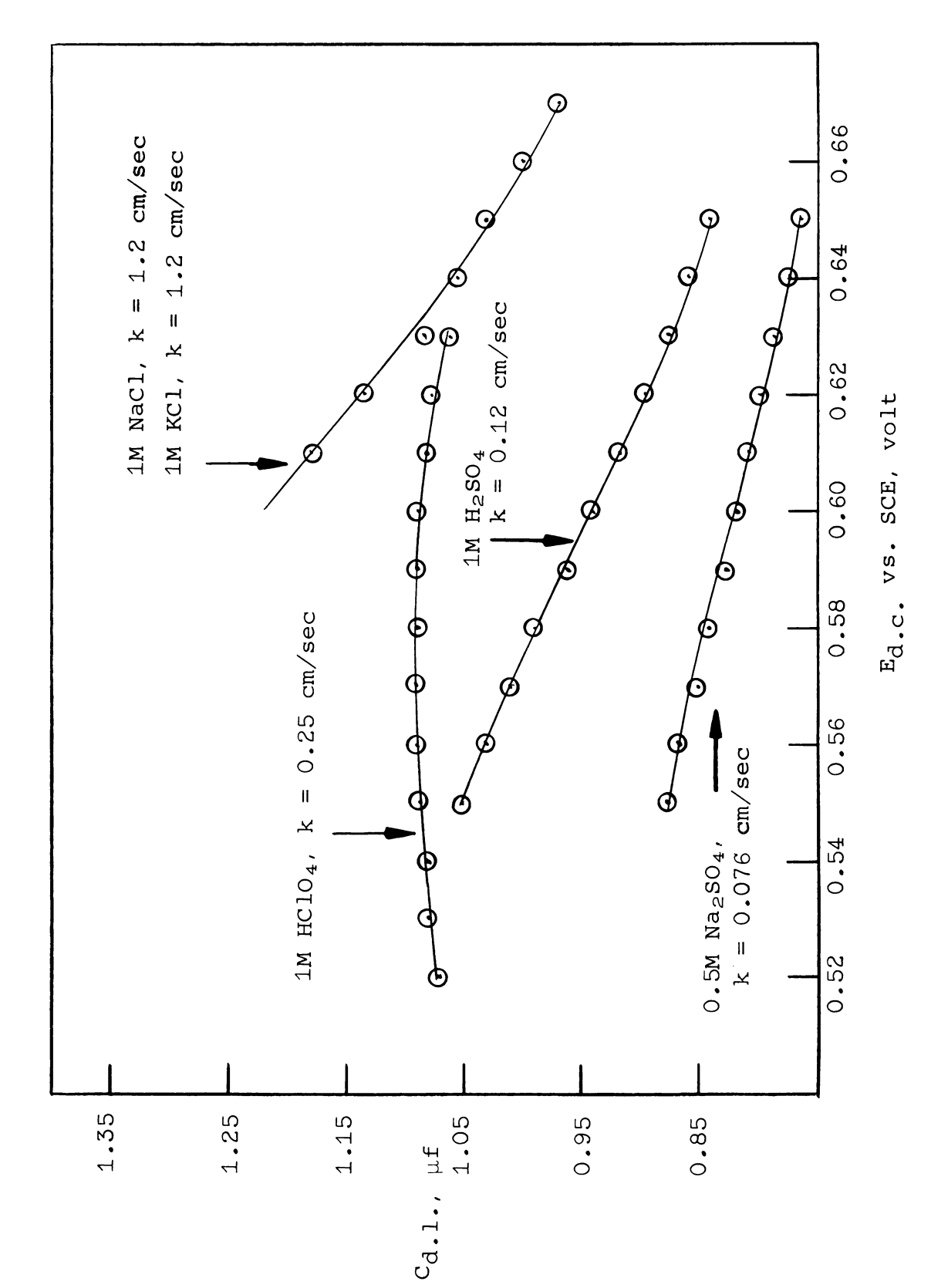
Tabulation of Heterogeneous Rate Constants and Transfer Coefficient. Values Determined by Various Investigators Table VIII.

0.5M Na ₂ SO ₄	0.026 0.085 0.042 0.045	0.25		41
0.5M Na ₂ SO ₄	0.085 0.042 0.045 0.25		voltage step	1
0.5M Na ₂ SO ₄ 0.5M Na ₂ SO ₄ 0.5M Na ₂ SO ₄	0.042	0.12	faradaic impedance	41
0.5M Na ₂ SO ₄ 0.5M Na ₂ SO ₄ 0.5M Na ₂ SO ₄	0.045	0.17	faradaic impedance	41
0.5M Na ₂ SO ₄ 0.5M Na ₂ SO ₄	0.25	0.22	current step	41
0.5M Na2SO4		 	a.c. polarography	3
	0.075	0.22	potential step method	28
0.5M Na ₂ SO ₄	 	0.38	a.c. polarography	വ
1.0M Na ₂ SO ₄	0.23-0.25	 	cyclic voltammetry	32
1.0M Na ₂ SO ₄	~0.3	1	a.c. polarography	10
1.OM KNO3	9.0		faradaic impedance	41
1.0M KNO_3	71.0	1	a.c. polarography	35
1.0M KNO_3	76.3	0.15	faradaic rectification	41
1.OM KNO3	~0.4	!!!!	a.c. polarography	10
1.0M KC1	!!!!!!!!!!!!!!!!!!!!!!!!!!!!!!!!!!!!!!!	0.45	a.c. polarography	24
1.0M KC1	2.9	0.78	faradaic rectification	41
0.5M KC1	~1.5	!!!!!!!!!!!!!!!!!!!!!!!!!!!!!!!!!!!!!!!	faradaic impedance	41
0.1M KC1		0.50	a.c. harmonic	41
1M HCl	9.0	!	a.c. polarography	10
0.5M HCl	0.165	0.41	a.c. polarography	24
0.5M HC1	0.5	 	a.c. polarography	10
1.0M HClO4	1.8	0.08	faradaic rectification	41
1.0M HClO4	9.0	!	cyclic voltammetry	32
1.0M HClO4	0.35	0.14	faradaic impedance	9

aReference 41 is a compilation of kinetic parameters by Tanka and Tamamuski from various investigators.



Variation of double-layer capacitance with changing applied d.c. potential for various supporting electrolytes. Figure 18.



Variation of double-layer capacitance with changing applied d.c. potential for various supporting electrolytes. Figure 19.

The capacity of the double-layer at a constant d.c. potential can be affected by adsorption of reactants, products, and supporting electrolyte. Since k_h is relatively constant with changing Cd(II) concentration, it is usually assumed (9) that adsorption of the electroactive species is negligible.

In a recent monograph Delahay (14) shows that the parameter, $k_h^{'}$ should decrease with increasing supporting electrolyte concentration, and that specific adsorption of an anion on the electrode should increase the charge-transfer rate for reduction of a non-adsorbed cation and be decreased by the presence of specifically adsorbed cation. The above generalities however are often complicated by formation of complexes between the reducible cations and anions in solution.

Delahay (15) lists the amounts of specifically adsorbed anions on mercury at a constant d.c. potential. The degree of adsorption is

$$C1^- > NO_3^- > SO_4^-$$

while Grahame (23) in earlier work determined the order to be

$$C1^{-} > NO_{3}^{-} > C1O_{4}^{-}$$
.

No comparison of the relative adsorbabilities of ClO_4 to SO_4 could be found in the literature. In the d.c. potential region investigated, there is little probability that any significant amount of cation is being adsorbed on the electrode.

,		

From Figures 18 and 19, it can be seen that the order of capacitance of the double-layer for the anions of the supporting electrolyte solutions is

$$Cl^- > NO_3^- > ClO_4^- > SO_4^-$$
.

The values of $k_h^{'}$ for these media decrease in this same order. These results provide experimental evidence to substantiate the statements made by Delahay (14) that the adsorption of anions increases the rate of reduction of non-adsorbed cations.

Limited evidence is also presented to support the statement that increasing the concentration of supporting electrolyte should decrease the rate constant. In Table VI this trend becomes apparent. The value of k_h in 0.5M Na₂SO₄ is 0.076 cm/sec while in 1M Na₂SO₄ it is 0.063 cm/sec. Also in 0.5M H₂SO₄ it is 0.14 cm/sec while in 1M H₂SO₄ it is 0.12 cm/sec. Admittedly the significance of these differences in k_h may be open to question until work at higher and lower supporting electrolyte concentrations is carried out.

SUGGESTED FURTHER WORK



On examining the experimental results obtained with the instrument certain experiments should be undertaken.

Since the charge-transfer rate in chloride media appears to be so rapid and so slow in sulfate, various small concentrations of chloride could be added to the sulfate medium to determine whether the rate could be enhanced. The effect of the added chloride in the double-layer capacity could also be determined.

The effect of supporting electrolyte concentration on the charge-transfer rate should be examined.

It would be of interest to duplicate the experiments of the completed study with increased a.c. potential amplitudes to test at which amplitude level the rate constant becomes amplitude dependent.

SUMMARY AND CONCLUSIONS

An improved a.c. polarograph was constructed. Its general features are those of an instrument constructed by Smith (37). The following modifications were introduced.

A low-gain operational amplifier was interposed between the cathode bias of the potentiostat and the tuned amplifier. This assured maintaining a virtual ground at the input of the cathode bias so that a 5mv a.c. potential could be accurately placed between the reference and at the indicating electrodes at all frequencies employed.

Electrochemical kinetic parameters are difficult to evaluate from alternating current measurements. These parameters are more simply and directly evaluated from phase-angle measurements. An improved phase-angle measuring circuit was designed and incorporated.

With a test RC series circuit constructed from components with 1% tolerance, measured phase-angles agreed with calculated values to within 1% through the frequency ranges of 30 to 250cps and 300 to 1200cps.

Transfer coefficients evaluated for the reduction of 1.0mM Cd(II) at the dropping mercury electrode at 24 \pm 1°, for the following supporting electrolytes, 0.5M Na₂SO₄, 1.0M Na₂SO₄, 0.5M H₂SO₄, 1.0M H₂SO₄, 1.0M NaClO₄, 1.0M HClO₄, 1.0M KNO₃, 1.0M HCl, 1.0M NaCl, 1.0M KCl were: 0.21, 0.20, 0.27, 0.24, 0.31, 0.26, 0.50, 0.42, 0.46, 0.44 respectively and the values for the heterogeneous rate constants, $k_h^{'}$, for the same order of the above supporting electrolytes were:

0.076, 0.063, 0.14, 0.12, 0.34, 0.25, 0.63, 0.94, 1.2, 1.2, cm/sec respectively.

Straight line cot $\phi - \omega^2$ plots, with intercepts cot $\phi = 1$, extrapolated to zero frequency, were obtained through the frequency range 30-1100cps for all supporting electrolytes containing Cd(II).

Linearity in the above plot, and agreement between experimental and calculated cot ϕ values, employing an appropriate equation derived for the electrode process

$$0 + ne \longrightarrow R$$

is evidence that the electrode process is only diffusion and charge-transfer controlled.

The order of double-layer capacitance for the anions of the various supporting electrolyte solutions at a d.c. potential of 0.6v vs. SCE was as follows:

$$C1^- > NO_3^- > C1O_4^- > SO_4^-$$
.

This order parallels the order of adsorbabilities of the above anions on mercury.

The decrease in heterogeneous rate constants for the reduction of Cd(II) in the above supporting electrolytes parallels the decrease in double-layer capacitance.

LITERATURE CITED

- 1. Bauer, H. H., Elving, P. J., J. Am. Chem. Soc. <u>30</u>, 341 (1958).
- 2. Ibid., 82, 2091 (1960).
- 3. Ibid., 82, 2094 (1960).
- 4. Bauer, H. H., Elving, P. J., Anal. Chem. 30, 334 (1958).
- 5. Ibid., 30, 341 (1958).
- 6. Biegler, T., Laitinen, H. A., Anal. Chem. 37, 572 (1965).
- 7. Bjerrum, J., Schwarzenbach, G., Sillen, L., Stability Constants, Part II Inorganic Ligands, pp. 55, 84, 103, 111, The Chemical Society London, 1958.
- 8. Breyer, B., Bauer, H. H., Alternating Current Polarography and Tensammetry, in Chemical Analysis, P. J. Elving and I. M. Kolthoff, eds., Vol. 13, pp. 1-25, Interscience, New York, 1963.
- 9. Ibid., p. 150.
- 10. Breyer, B., Bauer, H. H., Australian J. Chem. 9, 425 (1956).
- 11. Breyer, B., Hacobian, S., ibid., 8, 322 (1955).
- 12. Deford, D. D., <u>Stabilized Follower Amplifier</u>, Applications Bulletin, G. A. Philbrick Researches, Inc., Boston, Mass.
- 13. Delahay, P., New Instrumental Methods in Electrochemistry, p. 48, Interscience, New York, 1954.
- 14. Delahay, P., <u>Double Layer and Electrode Kinetics</u>, p. 206, Interscience, New York, (1965).
- 15. Ibid., p. 61.
- 16. Delahay, P., Adams, T. J., J. Am. Chem. Soc. <u>74</u>, 5740 (1952).
- 17. Delmastro, J. R., Smith, D. E., J. Electroanalyt. Chem. 9, 192 (1965).
- 18. Ibid., Anal. Chem. 38, 169 (1966).
- 19. Ershler, B., Faraday, Soc. Discussion 1, 269 (1947).
- 20. Frischmann, J. K., unpublished work.

- 21. Glasstone, S., Laidler, K. J., Eyring, H., <u>The Theory of Rate Processes</u>, pp. 575-77, McGraw-Hill, New York, 1941.
- 22. Grahame, D. C., J. Am. Chem. Soc. 63, 1207 (1941).
- 23. Grahame, D. C., Chem. Rev. 41, 441 (1947).
- 24. Head, W. F., Anal. Chim. Acta 23, 297 (1960).
- 25. Kelley, M. T., Jones, H. C., Fisher, D. J., Anal. Chem. 31, 488 (1959).
- 26. Koutecky, J., Chem. Listy 47, 323 (1953).
- 27. Lingane, J. J., Loveridge, B. A., J. Am. Chem. Soc. <u>72</u>, 439 (1950).
- 28. Lingane, P. J., Christie, J. H., J. Electroanalyt. Chem. <u>10</u>, 1284 (1965).
- 29. Matsuda, H., Z. Elektrochem. <u>61</u>, 489 (1957).
- 30. Ibid., 62, 977 (1958).
- 31. Müller, R. H., Garman, R. L., Droz, M. E., Petras, J., Ind. Eng. Chem. 10, 339 (1938).
- 32. Nicholson, R. S., Anal. Chem. <u>37</u>, 1351 (1965).
- 33. Operational Amplifier Symposium, Anal. Chem. 35, 1770-1845 (1963).
- 34. Randles, J. E. B., Faraday Soc. Discussion $\underline{1}$, 11 (1947).
- 35. Randles, J. E. B., Somerton, K. W., Trans. Faraday Soc. 48, 951 (1952).
- 36. Schwarzenbach, G., Complexometric Titration, pp. 55, 83-86, Interscience, New York, 1957.
- 37. Smith, D. E., Anal. Chem. 35, 602 (1963).
- 38. Ibid., 35, 1811 (1963).
- 39. Ibid., <u>36</u>, 962 (1964).
- 40. Tachi, I., Senda, M., Bull. Chem. Soc. Japan <u>28</u>, 632 (1955).
- 41. Tanaka, N., Tamamushi, R., Electrochim. Acta $\underline{9}$, 963 (1964).



